

# Capacity Analysis of Traffic-Actuated Intersections

by

Zhili Tian

Eng.B. in Civil Engineering (1988)  
Tsinghua University, Beijing, P. R. China

Submitted to the Department of Civil and Environmental Engineering in partial fulfillment of the requirements for the degree of

Master of Science in Transportation

at the

MASSACHUSETTS INSTITUTE OF TECHNOLOGY

September 2002

© 2002 Massachusetts Institute of Technology. All rights reserved.

Signature of Author .....  
Department of Civil and Environmental Engineering  
August 16, 2002

Certified by .....  
Moshe E. Ben-Akiva  
Edmund K. Turner Professor of Civil and Environmental Engineering  
Thesis Supervisor

Certified by .....  
Haris N. Koutsopoulos  
Operations Research Analyst  
Volpe National Transportation Systems Center  
Thesis Supervisor

Accepted by .....  
Oral Buyukozturk  
Chairman, Departmental Committee on Graduate Studies



# Capacity Analysis of Traffic-Actuated Intersections

by

Zhili Tian

Submitted to the Department of Civil and Environmental Engineering on August 16, 2002 in partial fulfillment of the requirements for the degree of Master of Science in Transportation

## Abstract

This thesis proposes two models that estimate the capacity of an intersection with actuated control. The capacity of an approach to or a lane group of the intersection is a function of the saturation flow rate, the green time allocated to this approach or lane group, and the cycle length of the intersection. The Minimum Delay Model estimates the green times and the cycle lengths from flow rates, minimizing the total delay at the intersection. Parameters, the ratio of green extension period to queue service time specific to each approach or lane group, are introduced into this model. The parameters depend on the distribution of arrivals of vehicles at the intersection. The Hybrid Model combines the deterministic queuing model that estimates the queue service time and a theoretical model that estimates the green extension period from the unit extension, the flow rate, the speed limit of the approach, and the detector length. A method converting the left-turn traffic volume to equivalent through volume is developed. The method is applied to estimating the capacity of intersections with permitted left-turn phases. The Minimum Delay Model and the Hybrid Model are validated at the intersection level by comparing the estimations of effective green ratios with those simulated by MITSIM-Lab. These two models are also validated at the network level with real data from Irvine, California. The results show that both the Minimum Delay Model and the Hybrid model are appropriate for estimating capacity of intersections with actuated control. The Minimum Delay Model is also suitable for estimating capacity of intersections with adaptive control. The Emulation Model is applicable to off-line mesoscopic dynamic traffic assignment.

Thesis Supervisor: **Moshe E. Ben-Akiva**

Edmund K. Turner Professor of Civil and Environmental Engineering

Thesis Supervisor: **Haris N. Koutsopoulos**

Volpe National Transportation Systems Center



## **Acknowledgment**

I am indebted to a great number of people who generously offered advise, encouragement, inspiration, and friendship throughout my time at MIT.

I hold my utmost respect and sincere gratitude to my advisor, Prof. Moshe Ben-Akiva and Dr. Haris Koutsopoulos. I thank Moshe for sharing his knowledge, for support, for the opportunities he has provided me, for forcing me dig deeper into my research, his encouragement, and his invaluable ideas. I thank Haris for sharing his knowledge, his friendship, his guidance, his support, his patience, and his selfless commitment.

I thank my fellow students at ITS lab. Thanks to Kunal Kunde, Rama Balakrishna, Srinivasan Sundaram and for their technical aid, friendship and their work on DynaMIT. Thanks to everyone else in the ITS lab for their friendship and kindness.

I thank the faculty and staff of CTS for their dedicated and kindness. Special thanks to Leanne Russell for her kind support.

Finally, my greatest thanks and appreciation go to my family. I thank my family for their permanent love and support. I realize how lucky I am to have them.



## Contents

<b>ABSTRACT.....</b>	<b>3</b>
<b>ACKNOWLEDGEMENT.....</b>	<b>5</b>
List of Tables .....	9
List of Figures .....	10
<b>CHAPTER 1 INTRODUCTION.....</b>	<b>11</b>
1.1 Scope of the Thesis.....	12
1.2 Contributions.....	12
1.3 Thesis Organization.....	12
<b>CHAPTER 2 LITERATURE REVIEW.....</b>	<b>14</b>
2.1 Introduction .....	14
2.2 Pretimed Controls.....	14
2.3 Actuated Controls.....	15
2.3.1 NEMA Controller .....	16
2.3.2 Timing Characteristics.....	18
2.4 Adaptive Control .....	20
2.4.1 Traffic-Responsive System (SCOOT) .....	21
2.4.2 Optimized Policies for Adaptive Control .....	23
2.5 Methods for Estimating the Capacity of Traffic-Actuated Intersections .....	25
2.5.1 Allsop's Method .....	26
2.5.2 Daganzo's Method.....	27
2.5.3 Highway Capacity Manual Methodology .....	29
2.5.4 Traffic Control System Handbook.....	33
<b>CHAPTER 3 CAPACITY ESTIMATION OF APPROACHES TO ISOLATED INTERSECTIONS WITH TRAFFIC-ACTUATED CONTROL.....</b>	<b>34</b>
3.1 The Minimum Delay Model.....	34
3.1.1 Assumptions .....	34
3.1.2 Determination of the Intersection Capacity by Minimizing the Total Delay.....	35
3.1.3 Expressions of Cycle Length and Green Times.....	39
3.1.4 Reformulation of the Optimization Problem in terms of $\alpha_i$ and $y_i$ .....	43
3.1.5 Comments on the Minimum Delay Model .....	45
3.2 The Hybrid Model.....	45
3.3 Treatment of Left-turn flow Rates in Capacity Estimation .....	47
<b>CHAPTER 4 IMPLEMENTATION OF CAPACITY ESTIMATION MODELS IN DYNAMIT 49</b>	
4.1 Introduction to DynaMIT .....	49
4.2 Implementation of the Minimum Delay Model and the Hybrid Model .....	51
4.2.1 Averaging the Lane Group Capacities.....	52
4.2.2 Input Data for the Capacity Estimation Models .....	53
4.3 Imposing Lower Bound on Green Times and Initial Lane Group Capacities .....	53
<b>CHAPTER 5 VALIDATION OF THE PROPOSED MODELS.....</b>	<b>54</b>
5.1 Validation of the Proposed Models at Intersection Level .....	54
5.1.1 Introduction to the Two Intersections.....	54
5.1.2 Comparison of the Proposed Models with those from TCS Handbook.....	57
5.1.3 Comparison of the Green Times Estimated by Proposed Models with those simulated by MITSIM-Lab at An Intersection with Eight Protected Phases .....	59

5.1.4 Comparison of the Green Time Estimations by Different Models at An Intersection with Permitted Left Turn Phases .....	64
5.2 Validation of the Capacity Estimation Models at Network Level.....	67
5.2.1 Introduction.....	67
5.2.2 Comparison of the Field Observations and the Simulated Flows.....	68
5.2.3 Error Statistics.....	69
5.3 Validation Conclusion.....	70
<b>CHAPTER 6 CONCLUSION AND FUTURE STUDY .....</b>	<b>71</b>
6.1 Conclusion.....	71
6.2 Future Study .....	72
<b>APPENDIX A GREEN TIMES AND CYCLE LENGTH FOR N PHASES.....</b>	<b>73</b>
1. The Relationship between $\lambda_2$ and $y_2$ for Approach 2 .....	73
2. The Cycle Length and Green Times for An Intersection with n Phases .....	73
3. Correctness of the Minimum Delay Model .....	75
<b>APPENDIX B .....</b>	<b>78</b>
1. Representation of $\bar{C}$ in Terms of $\alpha_1$ , $\alpha_2$ , $y_1$ , and $y_2$ .....	78
2. Representation of $d_q$ in Terms of $\alpha_1$ , $\alpha_2$ , $y_1$ , and $y_2$ .....	78
3. Representation of $d_r$ in Terms of $\alpha_1$ , $\alpha_2$ , $y_1$ , and $y_2$ .....	79
<b>APPENDIX C INPUT DATA OF CAPACITY ESTIMATION .....</b>	<b>81</b>
1. Determining Protected Left-turn or Permitted Left-turn Phases .....	81
2. Preparation of Input Data for Actuated Control .....	82
<b>BIBLIOGRAPHY.....</b>	<b>84</b>

**List of Tables**

Table 5-1 Saturation Flow Rates (vphg).....	56
Table 5-2 Saturation Flow Rates (vphg).....	57
Table 5-3 Comparison of Timing Plans Estimated by Four Different Models.....	58
Table 5-4 Flow Rates into the Intersection.....	61
Table 5-5 Effective Green Ratios Estimated by Different Models under Different Scenarios at Intersection of Irvine Center Dr and Laguna Cyn.....	61
Table 5-6 Flow Rates into the Intersection.....	64
Table 5-7 Comparison of Effective Green Ratios Estimated by Different Models under Different Scenarios at the Intersection with Permitted Left-turn Phases.....	65

## List of Figures

Figure 2.1 Four-phase Controller Diagram	16
Figure 2.2 Eight-phase (dual-ring) Controller Diagram	17
Figure 2.3 Phase Order for Dual-ring Controller	17
Figure 2.4 Actuated Phase Intervals	18
Figure 2.5 A Gap-reduction Function	20
Figure 2.6 The Actuated Traffic Signal Strategy under which Green Phases Terminate as soon as their Queues Vanish	28
Figure 2.7 Queue Accumulation Polygon Illustrating Green Time Computation	30
Figure 3.1 Intersection Layout	34
Figure 3.2 Signal Phases	35
Figure 3.3 Queue Accumulation Polygon	37
Figure 3.4 Traffic Actuated Control Strategy	40
Figure 4.1 Structure of DynaMIT	49
Figure 4.2 Simulation Process	50
Figure 5.1 Intersection of Irvine Center Dr and Laguna Cyn (Protected Phasing)	55
Figure 5.2 Intersection of Pasteur @ Laguna Cyn with One Permitted Left Turn Phase	55
Figure 5.3 Heavy Traffic Volume	62
Figure 5.4 Normal Traffic Volume	62
Figure 5.5 Light Traffic Volume	63
Figure 5.6 Heavy Traffic Volume	65
Figure 5.7 Normal Traffic Volume	66
Figure 5.8 Light Traffic Volume	66
Figure 5.9 Irvine Road Network	67
Figure 5.10 Field Observations v.s. Simulated Flows at Sensor 46	68
Figure 5.11 Field Observations v.s. Simulated Flows at Sensor 47	69
Figure 6.1 Interactions of Signal Control with DTA	72

## Chapter 1 Introduction

Urban traffic congestion is currently severe in most cities in the world and intelligent transportation systems are being designed to provide real-time control and route guidance to motorists to optimize traffic network performance. Actuated control policies and adaptive control strategies are becoming popular because of their potential to reduce delays at intersections. The advent of extremely fast methods of communication and computation in the past decade has created many new opportunities for controlling traffic on road networks. New control systems such as SCOOT, a traffic-responsive system, were developed in the U.K. for optimizing network traffic performance. New control algorithms such as Optimized Policies for Adaptive Control (OPAC), an on-line traffic signal timing optimization algorithm, were developed in the U.S.

Improvement of the traffic control of congested networks progresses slowly because of lack of understanding of the long-term dynamical system within which the traffic control system is embedded. In a congested network with traffic signals controlled automatically according to actuated or adaptive control policy, there are interactions between traffic and signal controls on the various streets. In reality, these interactions are often extremely complicated and their medium-term effects are hard to forecast. Dynamic traffic assignment (DTA) models have been applied to simulating the within-day dynamics of traffic, drivers' route choice, and dynamic traffic control.

In recent research of dynamic traffic assignment, researchers studied impacts of actuated control or responsive control on travelers' route choice and how drivers respond to traffic control. The current research on dynamic traffic assignment focuses on the realistic representation of the traffic network including formulating various actuated or adaptive traffic control. Most of the studies approximate the responsive traffic control by formulating delays on streets with actuated or adaptive traffic control. Since the real-world traffic controls are sophisticated, delay models cannot take into account the various control policies. In this research, we directly estimate the capacity of approaches to intersections with various traffic controls in dynamic traffic assignment.

The capacity of an approach to an intersection with traffic actuated or adaptive control is a function of the flow rates on approaches to the intersection. Since traffic demands are time-dependent, the capacities of intersections with signal control responding to traffic also vary. Intersection capacities estimated from historical demands do not reflect the variations of capacity within a day. Although capacity estimation for intersections with pre-timed control has been comprehensively studied and estimation models exist in the literature, those models cannot be used in estimating capacity of intersections with actuated or adaptive control. For instance, Webster's model is commonly used for designing timing plans of pretimed control. However, this model is not sensitive to the design parameters of actuated control (Courage, 1998). Therefore, the capacity estimation models for pretimed control cannot be used to determine the capacities of actuated intersections in dynamic traffic assignment (DTA).

The traffic controls are oversimplified in dynamic traffic assignment because the traffic-controlled intersections are usually treated as pre-timed. For example, DynaMIT uses the pre-determined approach capacities calibrated by the method of the Highway Capacity Manual (HCM) in traffic assignment. In order to capture the within-day dynamics of traffic, capacity estimation models for actuated or adaptive control should be developed and implemented in dynamic traffic assignment. The requirement of appropriately estimating capacities in DTA motivates this study.

### **1.1 Scope of the Thesis**

This thesis focuses on estimation of the capacity of approaches to intersections with actuated traffic control. Since the capacity of an approach is a function of the saturation flow rate, the green time allocated to this approach, and the cycle length of the intersection, models for determining green times and cycle lengths of the actuated intersections are developed in the thesis.

### **1.2 Contributions**

Major contributions of this research are as follows:

- Alternative models for capacity estimation
  - A model of capacity estimation, the Minimum Delay Model, is developed. The model estimates the green times and the cycle lengths from flow rates by minimizing the total delay of critical movements at an isolated intersection with actuated control.
  - Another model of capacity estimation, the Hybrid Model, is developed. The model for determining the capacity of actuated intersections in 2000 Highway Capacity Manual (HCM) is improved by estimating the queue service times with a deterministic queuing model. The iterative procedure for determining the queue service times is eliminated in the proposed model.
- A method, which converts left-turn traffic volumes to the equivalent through volumes at intersections with permitted left-turn phases, is developed. The method is applied to the estimation of capacity of intersections with actuated control.

### **1.3 Thesis Organization**

Chapter 2 provides an overview of pretimed, traffic actuated and adaptive control systems. This chapter also provides a review of various models of computing cycle lengths and green times of pretimed and actuated controls. Those models include the HCM model for actuated traffic control and the model presented by Daganzo (2000) for actuated control.

Chapter 3 proposes two models for capacity estimation. The green times are estimated as the queue service time and the green extension period from traffic volumes of the approaches to an isolated intersection in both models. The first model estimates the cycle length and green times for actuated control with the objective function that minimizes total delay of critical movements in a short time interval. The second model improves capacity estimation model for actuated control in HCM 2000. A method of adjusting left-turn volume is proposed for estimating the capacity of an intersection with permitted left-turn phases.

Chapter 4 proposes an iterative averaging method of updating capacities of approaches or lane groups in DTA.

Chapter 5 provides validation of the proposed models at both intersection level and at network level. Numerical comparison of the cycle lengths and the green times estimated by the two proposed models with those by the HCM model and by the model for actuated control in Traffic Control Systems (TCS) Handbook (1996). The effective green ratios determined by the two proposed models are compared with those simulated in Microscopic Traffic Simulator (MITSIM-Lab) at two intersections with actuated control in Irvine, CA. A real road network from Irvine, CA with two interstate highways and four arterial roads is used to validate the two capacity estimation models. Simulated traffic flow rates are compared with the field observations. The prediction errors of the simulated flow rates by DynaMIT with dynamic capacity estimation using the proposed models are compared with those by DynaMIT with static capacity estimation.

In Chapter 6, a conclusion is made of the applicability of the two proposed models for determining the intersection capacities. In addition, this chapter describes the future research for modeling capacity of intersections with adaptive control and combined model of DTA and adaptive traffic control.

## Chapter 2 Literature Review

### 2.1 Introduction

Traffic signal controls are implemented for reducing or eliminating conflicts at intersections. Signals accomplish this by allocating green times among the various users at the intersections. Signal controls vary from simple methods, which determine the timing settings on a time-of-day/day-of-week basis, to complex algorithms, which calculate the green time allocation in real time based on traffic volumes.

We introduce several basic timing parameters before discussing current signal control systems. A cycle is the time required for one complete sequence of signal indications. A phase is the portion of a signal cycle allocated to any combination of one or more traffic movements simultaneously receiving the right of way. Each phase is divided into a number of discretely timed intervals, which is a portion of the signal cycle during which all the signal indications remain unchanged, such as green, yellow change, and all red clearance. The split is the percentage of a cycle length allocated to each phase in a signal sequence (Kell and Fullerton, 1991).

### 2.2 Pretimed Controls

The pretimed control, which has fixed cycle lengths and preset phase intervals, operates according to a predetermined schedule. The pretimed controllers are best suited for locations with predictable volumes and traffic patterns such as downtown areas. Timing plans are usually selected on a time-of-day-of-week basis by means of time clocks. Although pre-timed controllers have a degree of flexibility in varying timing plan, they can cause excessive delay to vehicles where there exists a high degree of variability in the traffic flows because pre-timed control does not recognize or accommodate short-term fluctuations in traffic demand and uses timing plans determined from historical demands.

Pretimed signals assign the right of way to different traffic streams in accordance with a preset timing plan. The Webster method is used to determine the optimum cycle lengths. Since the actuated signals act as a fixed signal when all approaches are saturated, this method can be used to compute the cycle lengths and the green times for actuated traffic signals when the actuated controller operates as a pretimed signal. Webster (1958) has shown that minimum intersection delay is obtained when the cycle length is obtained by the equation

$$C = \frac{1.5L + 5}{1 - \sum_{i=1}^n y_i} \quad (2-1)$$

where:

$C$  = optimal cycle length (second);

$L$  = total lost time per cycle (second);

$y_i$  = the critical lane group volume ( $i$  th phase, vph) / saturation flow (vph);

$n$  = number of phases.

The total lost time is the time not used by any phase for discharging vehicles. Total lost time is given as

$$L = \sum_{i=1}^n l_i + R \quad (2-2)$$

where:

$l_i$  = lost time for phase  $i$ , which is usually 4 seconds;

$R$  = the total all-red time during the cycle.

The total effective green time, available per cycle, is given by

$$G_{te} = C - L. \quad (2-3)$$

To obtain minimum overall delay, the total effective green time should be distributed among the different phases in proportion to their  $y$  values to get the effective green time for each phase,

$$G_{ei} = \frac{y_i}{y_1 + y_2 + \dots + y_n} G_{te}. \quad (2-4)$$

The actual green time for each phase (not including yellow time) is obtained by

$$G_{ai} = G_{ei} + l_i - \tau_i \quad (2-5)$$

where  $\tau_i$  is yellow time for phase  $i$ .

### 2.3 Actuated Controls

An actuated signal operates with variable vehicular timing and phasing intervals that depend on traffic volumes. The signals are actuated by vehicular detectors placed in the roadways. The cycle lengths and green times of actuated control may vary from cycle to cycle in response to demands. Actuated controllers include semi-actuated, fully actuated, and density controllers.

In *semi-actuated operation*, the main street has a “green” indication at all times until a vehicle or vehicles have arrived on one or both of the minor approaches. The signal then provides a “green” phase for the side street that is retained until vehicles are served, or until a preset maximum side-street green is reached. Non-actuated phases may be coordinated with nearby signals on the same route, or they may function as an isolated control. Non-actuated phases usually operate with fixed minimum green times and may

be extended by using green time that is not used by actuated phases with low demand. That is, the green duration will be extended beyond the minimum green time until a vehicle actuates the detector on the side street. At a semi-actuated controlled intersection, detectors installed on the side street collect information for timing the signal.

In *fully actuated operations*, all signal phases are controlled by detector actuations. In general, each phase has a minimum green duration, but it also is shorter than the maximum green time. A phase in the cycle may be skipped entirely if no demand exists for that phase. The right of way does not return automatically to a specific phase under the fully actuated mode unless recalled by a special setting in the controller. That is, the controller shows green indication in the phase last served until conflicting demand appears.

In *density operations*, the controllers keep track of the number of arrivals and reduce the allowable gap according to several rules as vehicles show up or as time progresses. NEMA specifications allow gap reduction based only upon time waiting on the red (Mcshane, 1991). This type of controller also has a variable initial interval, thus allows a variable minimum green. Detectors are normally placed farther back of the intersection stopline, particularly on high-speed approaches to the intersection of major streets (Kell and Fullerton, 1991).

### 2.3.1 NEMA Controller

The National Electronic Manufacturers Association (NEMA) developed a functional standard in the traffic control field. NEMA controllers have similar functionality, which is widely used in the U.S. The controller operates based on phase diagrams that define the compatible phases and the order in which phases are displayed. An example of a simple four-phase diagram is shown in Figure 2.1. The east-west movements are served first, with the left turns in Phase 1 and with through and right movements in Phase 2, followed by the left and through/right movements for the north-south street in Phases 3 and 4, respectively. Each phase has a logic specified for its green timing, which may be pre-timed or demand responsive. The phase order is specified using the “conflict clearance” condition. In this example, Phase 2 will wait for Phase 1, Phase 3 for Phase 2, and Phase 4 for Phase 3, and Phase 1 for Phase 4, thus defining the proper phase order.

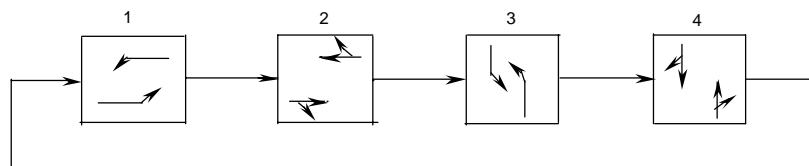


**Figure 2.1 Four-phase Controller Diagram**

An eight-phase controller that is more flexible in the phase progress is commonly used. It supports fully actuated control. Figure 2.2 shows the typical phase diagram for such a controller. The eight-phase controller operates two four-phase rings simultaneously,

allowing the rings to advance independently. For example, the controller will start by displaying Phases 1 and 5 because neither of Phases 1 or 2 conflicts with Phases 5 or 6, and then each phase can advance to its following phase when it is ready. The phase pairs of 1 & 5, 1 & 6, 2 & 5, and 2 & 6 are compatible and thus can be active simultaneously. The barrier that separates the primary street and cross-street movements imposes a restriction on the independence of the rings. Because all movements on one side of the barrier conflict with all movements on the other side, the rings must advance simultaneously across the barrier to prevent conflicting movements from being active simultaneously.

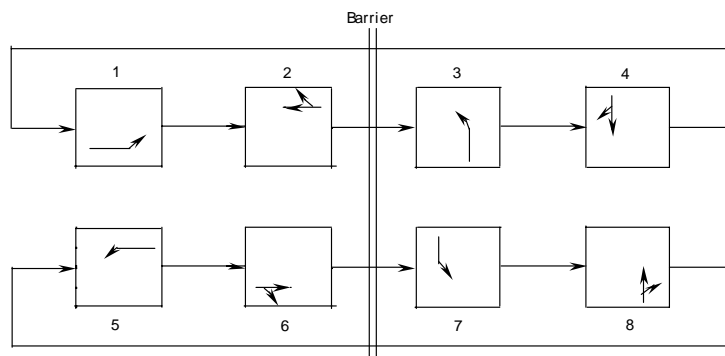


**Figure 2.2 Eight-phase (dual-ring) Controller Diagram**

Figure 2.3 shows the different phase sequences of the eight-phase controller. The phasing is similar to the four-phase controller with the addition of alternate transition phases where left and through movements may operate concurrently. Which transition phase used, if any, will depend on the ending times of Phases 1 and 5, determined either by preset timings or by vehicle actuations. Each phase has a preceding phase defined to specify the phase order. The barrier is modeled with the “complementary group” condition, which will hold a phase passively in green while another phase is still active. In the example above, Phases 2 and 6 are defined as complementary. This condition constrains their green intervals to end at the same time, assuring that the phase rings cross the barrier simultaneously. Phases 4 and 8 are similarly defined, modeling the return across the barrier to Phases 1 and 5.

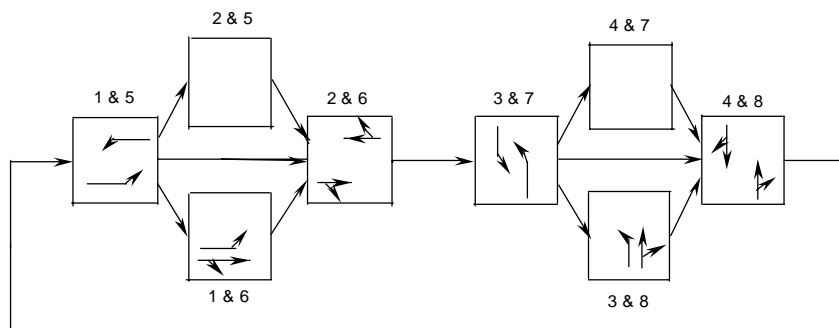


**Figure 2.3 Phase Order for Dual-ring Controller**

Modern traffic-actuated controllers usually implement a dual-ring concurrent phasing in which each phase controls only one movement, but two phases are generally being displayed concurrently. The term, “phase group”, is used in the analysis of intersection capacity, which is set of phases that are being displayed concurrently.

### 2.3.2 Timing Characteristics

In an actuated phase, there are three timing parameters: the minimum green interval, the unit extension, and the maximum green interval. These intervals are a function of the type and configuration of the detectors installed at the intersection. These three intervals are shown in Figure 2.4. This figure shows a case that the phase terminates before it reaches the maximum green period because there is no vehicular actuation in the last unit extension period.

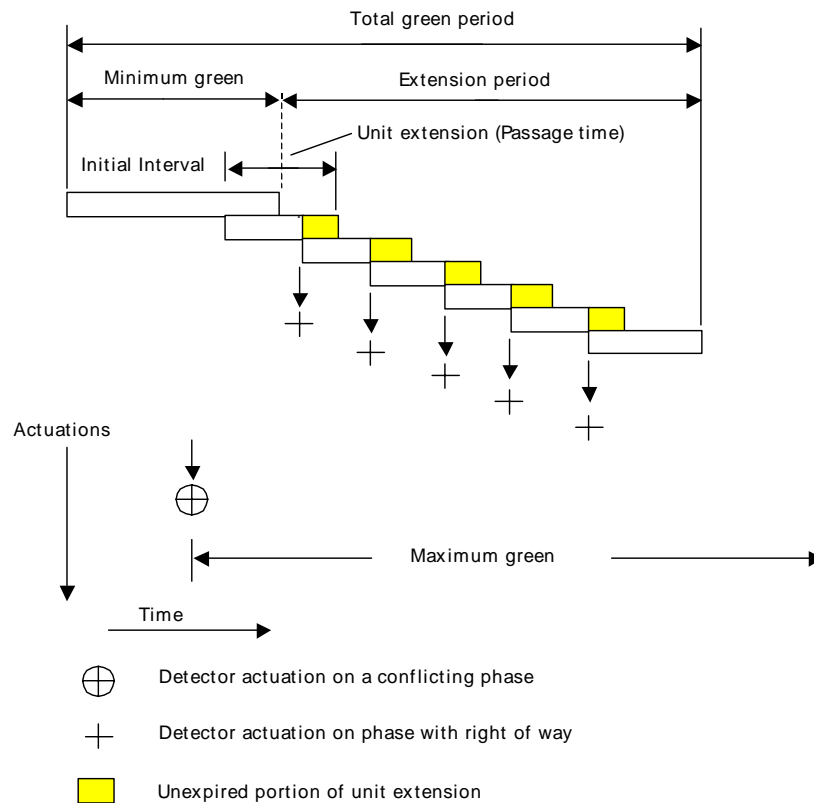


**Figure 2.4 Actuated Phase Intervals**

The *unit extension* is time by which a green phase could be increased during the extendable portion after an actuation on that phase (Garber and Hoel, 1997). It depends on the average speed of the approaching vehicles and the distance between the detectors and the stop line. The unit extension can be determined by the following equation

$$e_0 = \frac{S}{1.47v} \quad (2-6)$$

where:

$e_0$  = unit extension (seconds);

$v$  = average speed (mph);

$S$  = distance between detectors and stop line (ft).

*Initial interval* is the first portion of the green phase that is adequate to allow vehicles waiting between the stop line and the detector during the red phase to clear the intersection (Garber and Hoel, 1997). This time depends on the number of vehicles waiting, the average headway, and the starting delay. The initial interval can be obtained as

$$I = (hn + K_I) \quad (2-7)$$

where:

$h$  = average headway (seconds);

$n$  = number of vehicles between the detectors and the stop line;

$K_I$  = starting delay (seconds).

Suitable values for  $h$  and  $K_I$  are 2 seconds and 3.5 seconds, respectively.

*The minimum green interval* is the shortest time that should be provide for a green interval during any traffic phase. In basic design of actuated phase intervals, the minimum green interval equals the sum of the initial interval and the unit extension. In the advanced design of NEMA controller as shown in Figure 2.4 the minimum green interval may be less than the initial interval plus one unit extension.

*The maximum green interval* is the limit that a phase can hold green in the presence of conflicting demand. Normal range of maximum green is between 30 and 60 seconds depending on traffic volumes (Kell and Fullerton, 1991). Webster's model for pretimed controllers can be used to compute the maximum green interval. The computed green intervals are multiplied by a factor ranging between 1.25 and 1.50 to obtain the maximum green (Kell and Fullerton, 1991). NEMA specifies that the maximum green time not begin timing until there is a serviceable conflicting call. Therefore, a phase may remain green for some time before a conflicting demand appears that starts timing the maximum green.

*The logic of a typical semi-actuated control* has the following features (Kell and Fullerton, 1991):

The green duration for the side street starts with a predetermined initial interval, which is followed automatically by one unit extension  $e_0$ . If there is a side street vehicle actuating the detector during this unit extension, the green duration may be extended repeatedly in the same fashion until the maximum allowable green interval, is reached. If no single vehicle actuates the detector during a unit extension, the green duration will be terminated at the end of the unit extension.

According to this control logic, the average cycle lengths and cycle splits of a semi-actuated control are not affected by the traffic on the major street.

A fully actuated control does not distinguish between a major street and a side street. Every street is treated like a side street that is under a semi-actuated control. The control logic for each signal phase is the same as the one applicable to a side street under a semi-actuated control. Consequently, the resulting average cycle lengths and cycle splits depend not only on the signal timing plans but also on the traffic pattern in each phase.

In density mode, the unit extension time can also be set to vary as a function of the elapsed green time, usually reducing the extension time as the maximum time is neared. A variable extension length is often used because a long extension time is desirable at the start of the phase to ensure that vehicles are cross the intersection, while a shorter extension is desired near the end of the phase so that the phase is not extended unnecessarily (McShane et al., 1990). A typical “gap-reduction” function is show in Figure 2.5.

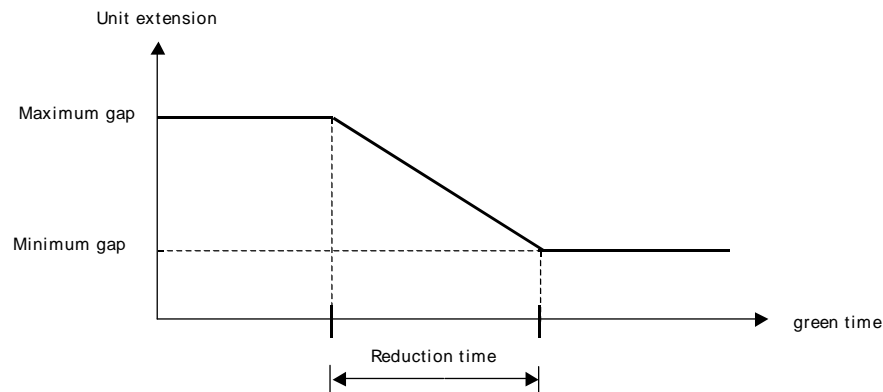


**Figure 2.5 A Gap-reduction Function**

Traffic-actuated controllers automatically determine cycle lengths and phase durations based on detection of traffic on the various approaches. The cycle lengths and green times are random variables, which depend on the real-time traffic demand. Therefore, the capacities of approaches to an intersection are random variables. A comprehensive review of the models estimating the timing plans and the approach capacities is presented in Section 2.5.

## 2.4 Adaptive Control

Adaptive control uses timing plans that are computed in real time, based on forecasts of traffic conditions. The detector observations are used as input into a prediction algorithm. This control is conceived as highly responsive with signal timing adjusted in small and frequent intervals. Examples of adaptive control systems are SCOOT (split, cycle and offset optimization technique) developed in the U.K., OPAC (Optimized Policies for Adaptive Control) developed in the U.S. and SCAT (Sydney Coordinated

Adaptive Traffic System) developed in Australia. We review the first two control systems in this section.

#### 2.4.1 Traffic-Responsive System (SCOOT)

SCOOT is a traffic-responsive urban traffic control system for optimizing network traffic performance. The systems monitor traffic conditions in a network by some form of detection and react to the information received by implementing appropriate signal settings. The SCOOT system adapts itself to traffic patterns and responds to traffic demands as they occur. The more recent version of the SCOOT system operates by interpreting comprehensive detector information online and monitors traffic flows continuously from on-street detectors. It uses this information to recalculate its traffic predictions every few seconds and then makes systematic trial alterations to current signal settings. New plans are continuously evolved in SCOOT system, which is valuable in central areas where congestion is high and flow patterns are complex and variable.

Inductive-loop detectors measuring vehicle presence (occupancy) are placed at the upstream end of each link in the SCOOT network and transmit the occupancy data to the central computer. The cyclic flow profiles for each link reveal the variation in traffic demand during each cycle. The detectors measure the cyclic flow profiles that are used to optimize signal coordination and for measuring and/or predicting queues, stops and congestion on each link. They are used during offset optimization to ensure good signal coordination.

The optimization model determines the signal timings that minimize a performance index (PI) for each SCOOT region, based on a weighted sum of delays and stops. For each traffic flow pattern and link-node arrangement a PI is calculated as (McDonald and Hounsell, 1991)

$$PI = \sum_{i=1}^N \left( W \omega_i d_i + \frac{K}{100} k_i S_i \right) \quad (2-8)$$

where:

$N$  = the number of links;

$W$  = the overall cost per average passenger car unit (pcu) equivalent hour of delay;

$K$  = the overall cost per 100 pcu stops;

$\omega_i$  = the delay weighting on link  $i$ ;

$d_i$  = the delay on link  $i$ ;

$k_i$  = the stop weighting on link  $i$ ; and

$S_i$  = the number of stops on link  $i$ .

The weighting factors balance the relative importance of queues and stops. A tendency exists to favor somewhat longer cycle times by using a heavy weight for stops (Roberston, 1986).

A SCOOT controlled network is divided into a number of regions. The SCOOT optimizer updates the traffic signal plan on a cycle-by-cycle basis. In doing this, the optimizer uses the previous cycle's signal settings as a seed in the search for new timings and makes minor alterations to these seed signal settings. The changes to the signal settings are made based on a restricted search for a minimum PI in the immediate vicinity of the seed signal settings, rather than by an exhaustive search for a global minimum PI (Rakha, 1995). The SCOOT adjusts signal timings in frequent small increments to match the latest traffic situation. These models ensure that queues cannot exceed a maximum queue value for each link.

*The cycle time optimizer* estimates the optimal cycle time for the region. The intersections in each region operate to their own common cycle time to ensure good signal coordination. For each region the model calculates the degree of saturation for all its nodes. It identifies the most critical node for each region and calculates the optimal cycle length which is used by all nodes. The cycle time is determined on the basis that the most heavily loaded intersection in the region should operate at a maximum degree of saturation of about 90%.

*The split optimizer* decides whether it will advance, postpone, or leave alone the green times for each stage. It seeks to balance the degree of saturation on all approaches and to avoid blocking-back. The green split is determined by minimizing the maximum degree of saturation on the approaches to that intersection. The level of congestion can also be included as an optimization criterion. In this calculation, the current estimates by SCOOT of the queue lengths, of any congestion measured on the approaches to the intersection, and of the constraints imposed by minimum green time is taken into account. Typically the lower bound might be about 30 or 40 seconds. The upper bound is set to give maximum traffic capacity but without unduly long red times. A maximum cycle time of 90 to 120 seconds is typically used in SCOOT.

*The offset optimizer* determines every cycle whether or not to alter all scheduled stage change times at an intersection. The sum of the PIs on all adjacent streets for the scheduled offset is compared with offsets that occur a few seconds earlier or later in determining the offset. The level of congestion can also be incorporated into the PI. The decisions of the offset optimizer are modified where congestion occurs; the purpose is to prevent queues of vehicles from growing to the point where upstream intersections are obstructed. Since congestion is more likely to occur on short sections of road, the offset optimizer acts to improve the coordination on the short streets by increasing queue on longer streets, which have space to store queues.

SCOOT is cycle-based and not fully reactive, and cannot respond to major discrete events appropriately in real time. It may also be slow in evolving with rapidly changing traffic demands, such as during the morning rush hour. It may therefore be providing slowly evolving "old" plans under such dynamic conditions. In addition, SCOOT is not efficient

algorithms for true real-time control that are compatible with a central control system. Further research on grouping signals into sub-areas may lead to new algorithms that are of sufficient generality and simplicity as to be attractive for on-line use. SCOOT has been developed for use when traffic demands are moderate to heavy. When traffic flows are low, it may not be necessary to run all the stages during every cycle time. However, SCOOT cannot skip traffic stages automatically.

#### 2.4.2 Optimized Policies for Adaptive Control

OPAC is an on-line traffic signal timing optimization algorithm, which was developed as a distributed system for traffic signal control without requiring a fixed cycle time. Signal timings are calculated to directly minimize performance measures, such as vehicle delays and stops, and are constrained by minimum and maximum phase lengths. The first version of OPAC solved the traffic control problem, using a dynamic programming algorithm. Each time interval is designated as a stage, which is typically five seconds. A “rolling horizon” concept was applied to the OPAC algorithm in order to use real time flow data. The horizon is typically equal to the average cycle length during which the OPAC calculates its switching decisions. The modified version was a simplification of the algorithm using dynamic programming. This version was reorganized for implementation in real time in a control system.

OPAC was improved by incorporating a traffic prediction model that predicts the traffic pattern over the entire stage. The horizon consists of a head and a tail portion. In the head portion of the horizon, the algorithm has available real-time vehicle arrival information. In the tail portion, the flows are estimated from previous measurements (Gartner, 1991). The detectors are placed well upstream of the intersection in order to obtain actual arrival information over the head period. Delay is calculated based on particular phase change decisions.

In OPAC, stops were included in the objective function, which is typically a linear combination of delays and stops, with the weight of stops relative to delay being one. In reality, this weight favors delay. At each individual intersection, phase plans are generated for future implementation based on current traffic conditions (i.e., current queues and expected arrivals) so as to minimize the objective function over a “decision horizon.” A phase plan is a sequential list of future switch points with each switch point representing the start of a certain phase at a specific time in the future. Traffic conditions are continuously monitored based upon vehicle detector and phase change information. The decision horizon typically ranges from less than thirty seconds to greater than two minutes in length. Phase plans are continually regenerated for the entire decision horizon but implemented only for the first three to five seconds. This “rolling-horizon process” allows signal timings to be constantly adapted to new traffic condition.

The optimization process is decomposed into  $N$  stages. The total number of stages  $N$  corresponds to the horizon length. At stage  $i$ , the input state vector is  $I_i$ , the arrivals vector is  $A_i$ , the output state vector is  $O_i$ , and the economic return output is  $r_i$ . A set of transformation functions is (Gartner, 1982):

$$O_i = T_i(I_i, A_i, r_i) \quad (2-9)$$

$$r_i = R_i(I_i, A_i, r_i) \quad (2-10)$$

The state of the intersection is characterized by the state of the signal and by the queue length on each of the approaches. The input decision variable indicates whether the signal is to be switched at this stage or to remain in its present state. The return output is the intersection's performance index. The optimization process minimizes the total performance index.

The dynamic programming optimization is carried out in backwards order, i.e., starting from the last stage and back-tracking to the first, at which time an optimal switching policy for the entire time horizon can be determined (Gartner, 1982). The recursive optimization function is given by the following equation,

$$f_i^*(I_i) = \min_{x_i} \{R_i(I_i, A_i, x_i) + f_{i+1}^*(I_i, A_i, x_i)\} \quad (2-11)$$

where the return at stage  $i$  is the queuing delay incurred at this stage:

$$R_i(I_i, A_i, x_i) = \sum_a (Q_i^a + A_i^a - D_i^a) = \sum_a Q_{i+1}^a \quad (2-12)$$

where:

$a$  = approach designation, by direction,  $a = N, S, E, W$ ;

$A_i^a$  = number of arrivals during stage  $i$ ;

$D_i^a$  = number of departures (discharges) during stage  $i$ ;

$Q_i^a$  = the queue length on the approach at the beginning of stage  $i$ .

The departure rate is a function of the state and decision variables (Gartner, 1982):

$$D = \begin{cases} 0 & \text{if } S^a = 1 \\ Q + A & \text{if } S^a = 0, Q + A \leq 2 \\ 2 & \text{if } S^a = 0, Q + A > 2 \end{cases} \quad (2-13)$$

where  $S^a$  is the signal status for approach  $a$ , defined as follows:

$$S^a = \begin{cases} 0 & \text{if } \text{green} \\ 1 & \text{if } \text{red} \end{cases} .$$

When the optimization is completed at stage  $i = 1$

$$f_1^*(I_1) = \min_{x_i} \sum_{i=1}^N R_i(I_i, A_i, x_i) = \sum_{i=1}^N r_i(I_i, A_i, x_i^*) \quad (2-14)$$

which is the minimized total delay over the horizon for a given input state  $I_l$ . Since the initial conditions at stage 1 are specified, the optimal policy is retraced by taking a forward pass through the stored tables of  $X_i^*(I_i)$ . The policy consists of the optimal sequence of switching decisions  $\{X_i^*, i = 1, \dots, N\}$  at all stages of the optimization process.

The OPAC strategy carries out sophisticated optimization in real time and adapts to varying traffic conditions. Field tests have shown that OPAC can provide significant benefits over well-timed actuated controllers. Because OPAC is not a traffic-driven controller, it forms a building block for a distributed intelligent traffic control system. Unlike conventional actuated control logic, the OPAC system can communicate with neighboring controllers so as to form a flexible coordinated traffic control system. OPAC uses the same performance measure as objective function for both off-peak traffic and peak traffic. A field test shows that when the observed volumes were extremely low the improvements were modest, because stops were not an OPAC measure of effectiveness in the first version of the system. OPAC adds to the optimization objective function a penalty, which is composed of the weighted sum of final queues on each approach. The penalty is added to minimize the final queues so that only minimal queues are transferred to the succeeding stage. At high level of volumes queues on some approaches may spread to the upstream intersection because OPAC system does not impose constraints on queues on approaches to an intersection. The unconstrained queues will reduce the capacity of the neighboring intersections.

## 2.5 Methods for Estimating the Capacity of Traffic-Actuated Intersections

The intersection capacity is a function of flow rates on approaches to an intersection for use in dynamic traffic assignment. The intersection capacity is represented by the capacities of approaches to the intersection. In general, the approach capacity is a function of the green time allocated to this approach, the cycle length of the intersection, the saturation flow rate of the approach, and the characteristics of the approaching flows. The capacity of approach  $a$  to the intersection can be determined as:

$$c_a = s_a (G / C)_a \quad (2-15)$$

where:

$c_a$  = the capacity of approach  $a$ , in vph;

$s_a$  = the saturation flow rate for approach  $a$ , in vphg;

$C$  = the cycle length of the intersection, in seconds; and

$G_a$  = effective green time for approach  $a$ , in seconds.

We review three models that estimate the green times and cycle lengths at an intersection with actuated control in this section.

### 2.5.1 Allsop's Method

Allsop (1972) formulated the capacity of a signalized intersection as a linear programming problem. The model can be used to design signal-timing plans by maximizing the capacity of approaches to an intersection and to determine approach capacities of the intersection as well. His results apply to both intersections in linked systems where traffic arrives mainly in platoons and isolated intersections where the traffic arrives at random because no assumption about the arrivals of traffic is made.

A part of the signal cycle in which one particular set of approaches has right of way is called a stage. At stage  $j$ , the proportion  $\Lambda_j$  of the cycle that is effectively green for approach  $j$  is given by

$$\Lambda_j = \sum_{i=0}^m (a_{ij} \lambda_i) \quad (2-16)$$

where:

$\lambda_j$  = the proportion of cycle that is effectively green for stage  $i$  ( $i = 1, 2, \dots, m$ );

$a_{ij} = 1$  if approach  $j$  has right of way in stage  $i$  ( $i = 1, 2, \dots, n$ ), and 0 if not; and

$a_{0j}$  = proportion of total lost time that is effectively green for approach  $j$  ( $j = 1, 2, \dots, n$ ).

The arrival rates on all approaches are multiplied by  $\mu$ . The queues and delays on all approaches will be acceptable if  $\Lambda_j \geq \mu b_j$  ( $j=1, 2, \dots, n$ ), i.e., if

$$\sum_{i=0}^m (a_{ij} \lambda_i) - \mu b_j \geq 0 \quad (j=1, 2, \dots, n) \quad (\text{approach capacity constraints}) \quad (2-17)$$

where:

$b_j$  = the smallest acceptable value of  $\Lambda_j$  when the arrival rate is  $q_j$ ;

$s_j$  = the saturation flow;

$p_j$  = adjustment factor of the  $s_j$ , the value is chosen by the engineer; and

$$b_j = q_j / p_j s_j. \quad (2-18)$$

In addition, the signal settings must satisfy the following constraints,

$$\lambda_i - k_i \lambda_0 \geq 0 \quad (i=1, 2, \dots, m) \quad (\text{minimum green constraints}); \quad (2-19)$$

$$\lambda_0 \geq k_0; \quad (2-20)$$

and

$$\sum_{i=0}^m \lambda_i = 1 \quad (\text{cycle time constraints}) \quad (2-21)$$

where:

$$k_i = g_{iM}/L; \quad (2-22)$$

$$k_0 = L/C; \quad (2-23)$$

where:

$g_{iM}$  = minimum green time for stage  $i$  ( $i = 1, 2, \dots, m$ );

$C$  = the maximum of specified cycle time; and

$k_0$  = the proportion of the cycle taken up by the lost time,  $L/C$ .

$\mu_j^*$ , ( $\mu_j^* = \Lambda_j/b_j$ ) is the largest value of  $\mu_j$  such that the delays and queues are acceptable. Then  $\mu_j^*q_j$  is the practical capacity of approach  $j$  when the proportion of the cycle of effective green for this approach is  $\Lambda_j$ .  $\mu^*$  can be solved as a linear programming problem:

Maximize  $\mu^*$

Subject to:

Equations (2-17), (2-19), (2-20), and (2-21).

Let  $p_j$  be the maximum degree of saturation that is acceptable on approach  $j$ . The approach capacity is defined as

$$c_j = p_j s_j \Lambda_j C \quad \text{for } j = 1, \dots, n. \quad (2-24)$$

Allsop's method (1972) does not provide a closed form expression of  $\mu^*$ . In order to get optimal  $\mu$ , one needs to solve the above linear programming problem. His formulation is appropriate for solving the signal design problem. However, Allsop's method is not applicable to estimation of the approach capacities in DTA since a linear program has to be solved for each intersection and time interval.

### 2.5.2 Daganzo's Method

Daganzo (2000) discussed an actuated control strategy that operates with cycles and phases close to the minimum while avoiding overflows. With this strategy traffic delay would be reduced by a factor of two, comparing with the pre-timed timing plan from Webster's model (Daganzo, 2000). The control strategy is: The actuated systems end the green phase on each approach as soon as its queue dissipates. Figure 2.6 illustrates this strategy by a simple intersection with two phases. The figure depicts two cumulative (virtual) arrival curves,  $V_1(t)$  and  $V_2(t)$ , starting at an instant ( $t = 0$ ) when the queue at Approach 2 has vanished and the queue of Approach 1 is  $Q_1(0) > 0$ . The saturation flows and the lost times for both approaches ( $s_i, L_i$ ) are known. The departure curves are constructed for any pair of  $V_i(t)$ 's. On the arrival and departure curves, arrowheads indicate the order in which points along the departure curves are obtained.

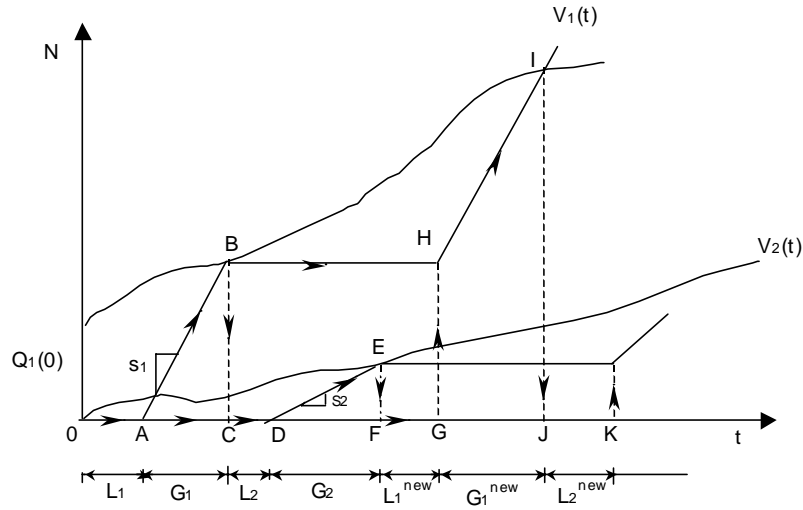


**Figure 2.6 The Actuated Traffic Signal Strategy under which Green Phases Terminate as soon as their Queues Vanish**

Daganzo (2000) derived the cycle length equation for this actuated control strategy. The following is the summary of the result. The average duration of a green phase for approach  $i$ , is  $\bar{G}_i$ . Each cycle has a total lost time  $L = L_1 + L_2$ .  $\bar{q}_i$  denotes average flow in an interval. The Cycle length is estimated as,

$$\bar{C} = L \left( 1 - \sum_i y_i \right)^{-1} \quad (2-25)$$

where  $y_i = \bar{q}_i / s_i$ .

The effective green ratio can be determined as,

$$\lambda_i = \bar{G}_i / \bar{C} = y_i \quad (i = 1, 2). \quad (2-26)$$

The above-mentioned actuated strategy is suitable for isolated intersections of major streets with under-saturated conditions. If traffic becomes over-saturated for an extended period, the strategy does not proactively allocate more green to the approach with the highest flow. Therefore, a long queue may be built up on the main street. In reality, the actuated signals do not work in the way as suggested by Daganzo. For instance, in the simple example illustrated in Figure 2.6, the Phase 1 terminates when the queue on Approach 1 dissipates. In practice, Approach 1 retains green time for an extended period until there is demand from Approach 2 or interarrival headway of traffic on Approach 1 is longer than the unit extension. Therefore, neither Equation (2-26) nor Equation (2-25) is appropriate for estimating green times of actuated control.

The above model also underestimates the average cycle length because it was essentially the cycle of an actuated signal for the queue to dissipate. If there is no recall from other phases, the green time on the last phase will extend to the maximum green time. The

actuated signals usually operate at cycle length between the minimum length and the maximum length. However, Daganzo's method can be used to estimate the queue service times of an actuated intersection, which is used to estimate the capacity of approaches to actuated intersection.

### 2.5.3 Highway Capacity Manual Methodology

#### **Pretimed Control**

Chapter 16 of the HCM 2000 describes a model for estimating the capacity and signal timing plans at a signalized intersection as a function of the traffic characteristics. The HCM suggests that the average cycle length and phase times may be approximated by assuming that the controller is effective in its objective of keeping the critical approaches nearly saturated. The cycle length is given by the following equation:

$$C = LX_c / [X_c - \sum (v/s)_{ci}] \quad (2-27)$$

where:

$C$  = cycle length, in sec;

$L$  = lost time per cycle, in sec;

$(v/s)_{ci}$  = flow ratios for critical lane group  $i$ ; and

$X_c$  = critical ratio of volume to capacity for the intersection.

The effective green time for a particular phase,  $G_i$ , is estimated with the following equation

$$G_i = \frac{v_i C}{s_i X_i} = \left( \frac{v}{s} \right)_i \left( \frac{C}{X_i} \right) \quad (2-28)$$

where:

$X_i$  = ratio of volume to capacity for lane group  $i$ ;

$v_i$  = demand flow rate for lane group  $i$ , vph;

$s_i$  = saturation flow rate for lane group  $i$ , vphg; and

$G_i$  = effective green time for lane group  $i$ , sec.

The average cycle length can be estimated using a user-specified  $X_c$ . The capacity of a lane group can be calculated by Equation (2-15) after the cycle length of the intersection and green time for lane group  $i$  are determined. This procedure is appropriate for estimating the lane group capacities of intersections with pretimed control.

#### **Traffic-Actuated Control**

The HCM 2000 describes a method for estimating the capacities of intersections with actuated control, which is sensitive to variations in design parameters. The models were developed based on the concept of queue accumulation polygon (QAP) which plots the

number of vehicles queued at the stop line over the cycle. Figure 2.7 depicts the QAP for a simple protected movement where the accumulation takes place on the left side of the triangle and the discharge takes place on the right side of the triangle. The duration of a green interval is determined by the length of the previous red interval and the arrival rates. The average green time of a phase is estimated as the sum of the queue service time and the phase extension period as shown in Figure 2.7.

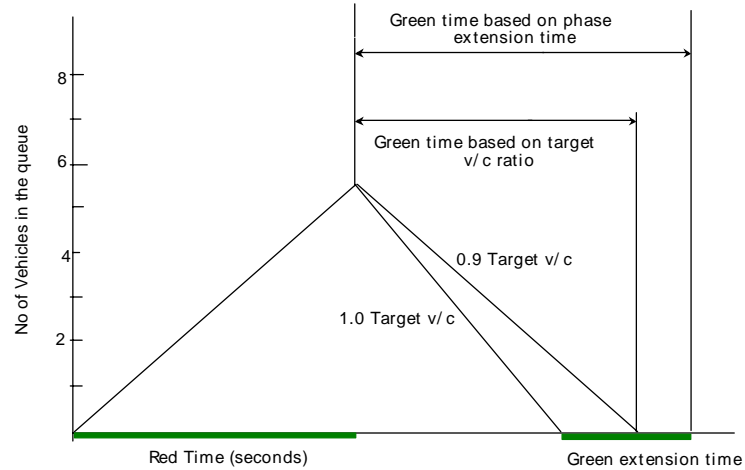


**Figure 2.7 Queue Accumulation Polygon Illustrating Green Time Computation**

The queue service time,  $G_q$ , is given by

$$G_q = f_q \frac{q_r r}{(s - q_g)} \quad (2-29)$$

where:

$q_r, q_g$  = red arrival rate (veh/sec) and green arrival rate (veh/sec), respectively;

$r$  = effective red time (sec);

$s$  = saturation flow rate (veh/sec);

$$f_q = 1.08 - 0.1(G / G_{max})^2 \quad (2-30)$$

where:

$G$  = the actual green (not including yellow time) (sec); and

$G_{max}$  = maximum green (sec).

The queue calibration factor,  $f_q$ , accounts for randomness in arrivals in determining the average queue service time.

The green extension period,  $G_e$ , is estimated by an analytical model, which was developed by Lin (1982) and improved by Akcelik (1994).  $G_e$  is estimated assuming that vehicle arrival according to the bunched exponential arrival headway distribution:

$$G_e = \frac{e^{\theta(e_0+t_0-\Delta)}}{\phi q} - \frac{1}{\theta} \quad (2-31)$$

where:

$q$  = the total arrival flow (veh/sec) for all lanes that actuate the phase under consideration;

$e_0$  = the unit extension time setting (sec);

$t_0$  = the duration during which the detector is occupied by a passing vehicle (sec),

$$t_0 = 0.68(L_d + L_v) / S_A \quad (2-32)$$

where:

$L_v$  = vehicle length, assumed to be 18 ft;

$L_d$  = detector length (ft);

$S_A$  = vehicle approach speed (mi/hr);

$\Delta$  = minimum arrival (intra-bunch) headway (seconds);

$\phi$  = proportion of free (unbunched) vehicles;

$\theta$  = a parameter calculated as:

$$\theta = \frac{\phi q}{1 - \Delta q} \quad (2-33)$$

The proportion of free vehicles in the traffic stream,  $\phi$ , is determined by the following relationship originally proposed by Brilton (1988)

$$\phi = e^{-b\Delta q} \quad (2-34)$$

where  $b$  is a bunching factor. HCM recommends parameter values as follows:

Single-lane case:  $\Delta = 1.5$  s and  $b = 0.6$

Multi-lane case (2 lanes):  $\Delta = 0.5$  s and  $b = 0.5$

Multi-lane case (3 or more lanes):  $\Delta = 0.5$  s and  $b = 0.8$

Green times are subject to the constraints of minimum and maximum green times, which are controller parameters. The capacity of lane groups of an intersection can be estimated by Equation (2-15) after the cycle length of the intersection and the green times are determined.

The method does not directly determine an average cycle length and green times, since the green time required for each phase depends on the green times required by the other phases. Thus, a circular dependency exists which should be solved iteratively. HCM recommends an iterative procedure to compute the queue service time and green extension period as follows:

The logical starting point for the iterative process involves the minimum times specified for each phase. If these times turn out to be adequate for all phases, the cycle length will simply be the sum of the minimum phase times for the critical phases. If a particular phase demands more than its minimum time, more time should be given to that phase. Thus, a longer red time must be imposed on all of the other phases. This, in turn, will increase the green time required for the subject phase.

Although the iterative procedure applicable to off-line capacity estimation, it is not applicable to the dynamic traffic assignment because of the real time nature of many applications. In addition to increasing the run time of DTA, the procedure usually does not converge to the actual green times. Therefore, a model that does not require iterative computation needs to be developed.

The following numerical example, which is used in the HCM 2000, demonstrates the estimation problem of the HCM method. Consider the intersection of two streets with a single lane in each direction. Each approach has identical characteristics, and carries 675 vehicles per hour with no left or right turns. The intersection is controlled by a two-phase actuated signal with one phase for the east-west movement and the other for north-south movement. The average headway is 2.0 seconds per vehicle and the lost time per phase is 3.0 seconds. The actuated controller settings are:

Initial interval:	10 seconds
Unit extension:	3 seconds
Maximum green:	46 seconds
Inter-green:	4 seconds

Using the HCM approach, the estimated value of green extension for each approach is 7 seconds since the approach flow rates are the same. The solution of the queue service time, a part of effective green time, is 39 seconds for each phase. The estimated cycle length is  $2 \times (39 + 7) + 2 \times 3 + 4 = 102$  seconds assuming that the total all-red time is 4 seconds. This result is slightly lower than the cycle length determined by Webster's model (For the demands at the intersection, the cycle length determined by Webster's model is 112 seconds).

In this example, the minimum phase time is, initial interval + unit extension + inter-green, which is  $10 + 3 + 4 = 17$  seconds for both phases. If a particular phase demands more than its minimum time, then more time must be given to that phase. Thus, a longer red time is imposed on all of the other phases. This, in turn, will increase the green time required for the subject phase. Since there is not any objective function and no

constraints in the iterative procedure, the cycle length converges at the one, which is longer than the actual cycle length.

#### 2.5.4 Traffic Control System Handbook

The Traffic Control System (TCS) Handbook (1996) provides a model for determining cycle length of actuated intersection, which is derived from Webster's model (1958), as follows,

$$C = \frac{1.3L}{1 - \sum_{i=1}^n y_i} \quad (2-35)$$

where  $y_i$  is the maximum ratio of flow rates to the saturation flow rates for approaches sharing the phase  $i$  and  $n$  is the number of phases. The cycle length estimated by this model is essentially 1.3 times the time interval for queues to dissipate. It cannot be justified that the actual length of a phase is 1.3 times the time for the queue to dissipate. In addition, the TSC model does not appropriately account for the mechanism of actuated control. Therefore, this model is not appropriate for capacity estimation for actuated intersections.

## Chapter 3 Capacity Estimation of Approaches to Isolated Intersections with Traffic-Actuated Control

In traffic-actuated control, controllers generate the green times and the cycle length on the basis of operating parameters and the vehicle demands registered by detectors. The capacities of approaches to an intersection are determined by the green times and the cycle length. Two capacity estimation models, which determine the approach capacities through the green times and the cycle length, are developed in this chapter. They are the Minimum Delay Model and the Hybrid Model.

### 3.1 The Minimum Delay Model

The capacities of approaches to an intersection are functions of green times and the cycle length. The model determines the green times and the cycle length by minimizing the total delay from flow rates at the intersection. A minimization model is introduced first with the objective function as the total delay at an actuated intersection. The green time for each phase consists of a queue service time and a green extension period. The ratio of the green extension period to the queue service time for each approach depends on the distribution of vehicle arrivals at the intersection. Expressions for the cycle length and the green times are developed as a function of flow rates, saturation flow rates, and the ratios of the green extension period to the queue service time.

#### 3.1.1 Assumptions

The discussion of capacity estimation of approaches to an intersection is based on the intersection illustrated in Figure 3.1. The figure shows the intersection of a two-lane road with another two-lane road. The flows of movements 1, 2, 3, and 4 are at moderate to high volume levels. The intersection is controlled by a two-phase, fully actuated traffic signal. The phase plan for this intersection is shown in Figure 3.2. During Phase 1, movements 1 and 3 are concurrently shown a green indication. Movements 2 and 4 are concurrently shown a green indication during Phase 2.

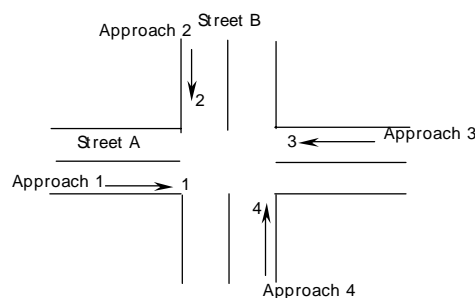


**Figure 3.1 Intersection Layout**

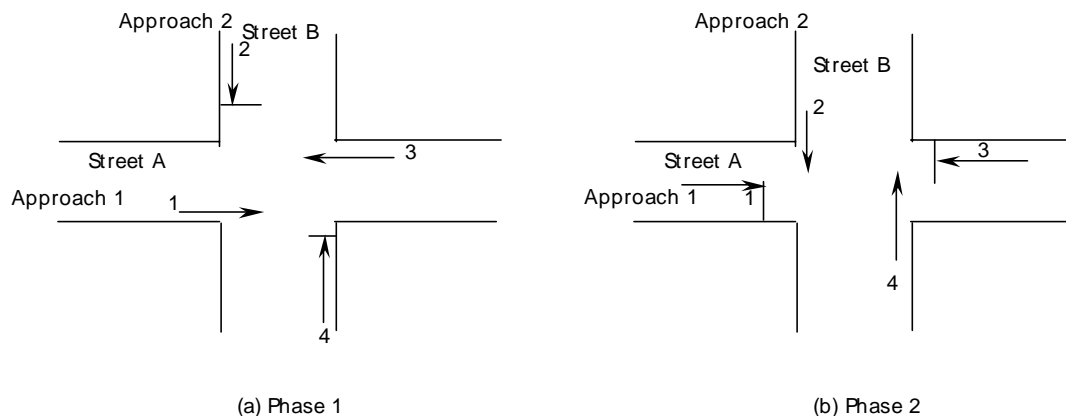


**Figure 3.2 Signal Phases**

The model assumes that demand is registered before the termination of the minimum green period, and therefore, the green extension period starts immediately after the expiration of the minimum green period. Thus, the green time estimated by this model is at least the minimum green time. The equations for estimating the green times and the cycle length are expressed in terms of effective green times rather than displayed green times.

Simplifying assumptions:

- 1) All approaches are unsaturated,  $\bar{q}_1 C < s_1 G_1$ ,  $\bar{q}_2 C < s_2 G_2$  with  $G_1 + G_2 + L = C$ , where  $\bar{q}_1$  and  $\bar{q}_2$  are the average flow rates on Approaches 1 and 2, respectively;
- 2) A queue develops during red indication, but it dissipates completely during green time; and
- 3) The traffic stream reaches uninterrupted status after the queue dissipates.

### 3.1.2 Determination of the Intersection Capacity by Minimizing the Total Delay

The intersection capacity is estimated by minimizing the total delay during a short time period,  $T$  that is chosen so that the flow rates are nearly constant. In simulation-based dynamic traffic assignment,  $T$  is usually the simulation interval so that the capacity estimation reflects the traffic dynamics during rush hour. Since the green times and the cycle length determine the capacity of an actuated intersection, we introduce a minimization problem that determines the green times and the cycle length.

If there is no randomness in traffic flows, the deterministic queuing delay agrees fairly well with actual delay. It is not so at higher values of flows where actual delays owing to the random nature of the arrivals are far in excess of values calculated from delay owing to the uniform arrivals. The total delay,  $d$ , is determined as the sum of the delay due to

uniform arrivals and the delay due to random arrivals. Researchers who studied the delay functions in the past four decades proposed several versions of delay functions. Although the most common models are different in form, they essentially include both a “uniform” or deterministic component and a “random” component. Most theoretical formulations of a delay relation have a correction term, which is based upon a set of simulation runs. For instance, Webster used a delay function, which includes uniform delay, random delay and an empirical term correcting the overestimation by the first two parts, to determine the cycle length formula for pretimed control. In fact, the net effect of the third term is a 5% to 15% decrease in the total (Webster, 1958). Webster’s delay model is as follows,

$$d = \frac{c(1-\lambda)^2}{2(1-\lambda x)} + \frac{x^2}{2q(1-x)} - 0.65 \left( \frac{c}{q^2} \right)^{\frac{1}{3}} x^{(2+5\lambda)} \quad (3-1)$$

where:

$\lambda = g/c$  , fraction of effective green time in cycle time;

$x = q/\lambda s$ , the degree of saturation;

$c =$  cycle time; and

$q =$  arrival rate (veh/hr).

We estimate the total delay by the uniform delay,  $d_u$ , and the random delay,  $d_r$ , as follows,

$$d = d_u + \beta d_r \quad (3-2)$$

where  $\beta$  is a random delay discount factor.

The choice of  $\beta$  affects the contribution of random delay to the total delay  $d$ . The parameter can be calibrated off-line based on the real data. If field observations of delay are not available, the HCM delay model can be used for estimating the green times and cycle length since the delay relation in the HCM was calibrated based upon a national intersection-delay database.

*The total uniform delay,  $d_u$ , during a cycle is determined based on the following queue accumulation polygon, which plots the number of vehicles queued at the stop line in one cycle. The queue accumulation and dissipation on Approach 1 are illustrated in Figure 3.3 (Symbols in the graph denote the average values in the time interval,  $T$ ). The accumulation takes place on the left side of the triangle (i.e., effective red) and discharge takes place on the right side of the triangle (i.e., a part of effective green during which a queue presents). In the figure,  $\bar{G}_{1,q}$ ,  $\bar{G}_{1,e}$ , and  $\bar{C}$  are the average queue service time, the average green extension period, and the average cycle length respectively. The average flow rate from Approach 1 and the saturation flow rate on Approach 1 are denoted as  $\bar{q}_1$  and  $s_1$ .*

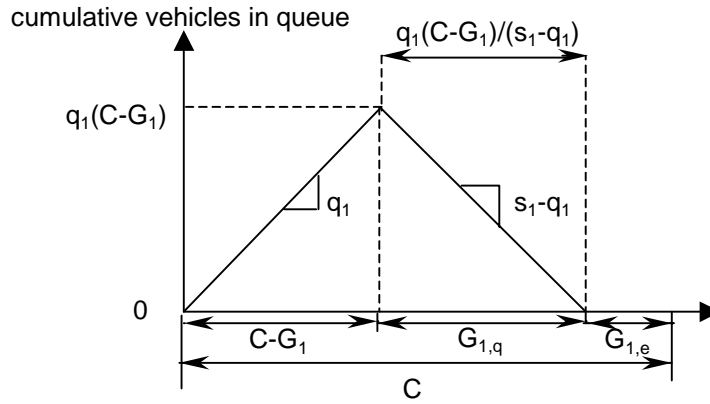


**Figure 3.3 Queue Accumulation Polygon**

Total uniform delay during  $\bar{C}$  on Approach 1,  $d_{u,1}$

$$d_{u,1} = \frac{1}{2} \bar{q}_1 (\bar{C} - \bar{G}_1) [(\bar{C} - \bar{G}_1) + \bar{G}_{1,q}] \quad (3-3)$$

where  $\bar{G}_{1,q} = \frac{\bar{q}_1 (\bar{C} - \bar{G}_1)}{s_1 - \bar{q}_1}$ .

Insert the above equation into Equation (3-3),

$$\begin{aligned} d_{u,1} &= \frac{1}{2} \bar{q}_1 (\bar{C} - \bar{G}_1)^2 \left[ 1 + \frac{\bar{q}_1}{s_1 - \bar{q}_1} \right] \\ d_{u,1} &= \frac{1}{2} \bar{q}_1 (\bar{C} - \bar{G}_1)^2 \frac{s_1}{s_1 - \bar{q}_1} \\ d_{u,1} &= \frac{1}{2} \bar{q}_1 (\bar{C} - \bar{G}_1)^2 \frac{1}{1 - y_1} \end{aligned} \quad (3-4)$$

where  $y_1 = \bar{q}_1 / s_1$ .

Similarly, we can derive the total uniform delay during  $\bar{C}$  on Approach 2,

$$d_{u,2} = \frac{1}{2} \bar{q}_2 (\bar{C} - \bar{G}_2)^2 \frac{1}{1 - y_2} \quad (3-5)$$

where  $y_2 = \bar{q}_2 / s_2$ .

The total uniform delay of critical movements in time interval,  $T$ , is

$$d_u = \frac{T}{C} \sum_{i=1}^2 \left[ \frac{1}{2} \bar{q}_i (\bar{C} - \bar{G}_i)^2 \frac{1}{1 - y_i} \right] \quad (3-6)$$

where the average number of cycles in the time interval,  $T$ , is given by  $T/\bar{C}$ .

The total random delay,  $d_r$ , at the intersection can be computed by the queuing model for exponential interarrival time and deterministic service time (M/D/1), since the saturation flow rate is a constant. The average delay due to random arrivals on approach  $i$  is:

$$d_{r,i} = \frac{\rho_i^2}{2\bar{q}_i(1-\rho_i)} \quad (3-7)$$

where:

$$\rho_i = \bar{q}_i / c_i = \frac{\bar{q}_i}{\frac{\bar{G}_i}{\bar{C}} s_i} = \frac{\bar{G}_i \bar{q}_i}{\bar{C} s_i} = \frac{\bar{G}_i}{\bar{C}} y_i, \text{ for } i = 1, 2; \quad (3-8)$$

$\bar{q}_i$  = the average flow rate on Approach  $i$  (veh/hr);

$d_{r,i}$  = the random delay on Approach  $i$  (hr/veh);

where:

$$c_i = \text{the capacity of approach } i \text{ (veh/hr), } c_i = \frac{\bar{G}_i}{\bar{C}} s_i;$$

$$y_i = \frac{\bar{q}_i}{s_i} \text{ for Approach } i. \quad (3-9)$$

The total delay due to random arrivals in the time interval,  $T$ , is

$$d_r = \sum_{i=1}^2 d_{r,i} \bar{q}_i T = \sum_{i=1}^2 \left[ \frac{\rho_i^2}{2(1-\rho_i)} \right] T. \quad (3-10)$$

The cycle lengths,  $\bar{C}$ , and green times,  $\bar{G}_i$ , are the solution to the following the following optimization problem,

$$\text{Minimize } d = d_u + \beta d_r \quad (3-11a)$$

Subject to:

$$G_{i,\min} \leq \bar{G}_i \leq G_{i,\max} \text{ for } i = 1 \text{ and } 2 \quad (3-11b)$$

where  $G_{i,\min}$  and  $G_{i,\max}$  are the minimum green time and the maximum green time for Phase  $i$ .

Although the uniform delay and the random delay expressions are derived based on a two-phase intersection, they are also the delay expressions for an n-phase intersection since both the delays for approach  $i$  are functions of the green time and the flow rate of approach  $i$  only. In the total uniform delay and total random delay expressions,

Equations (3-6) and (3-10) respectively, we add the delays from critical approaches from  $1$  to  $n$ .

### 3.1.3 Expressions of Cycle Length and Green Times

An actuated controller extends green times on the basis of the vehicle interarrival time on each approach. We will derive expressions for the green times and the cycle length for two-phase actuated control, taking into account of the green extension nature of actuated controllers. Appendix A gives the expression for green times and cycle length for an actuated controller with  $n$  phases. Figure 3.4 depicts two cumulative arrival curves for Approaches 1 and 2,  $V_1(t)$  and  $V_2(t)$  respectively under an actuated control strategy. At an instant ( $t = 0$ ) when the queue at Approach 2 has vanished the queue of Approach 1 is  $Q_1(0) > 0$ . The saturation flows and the lost times for Approaches 1 and 2 are  $(s_1, L_1)$  and  $(s_2, L_2)$  respectively. The departure curves are constructed for movements 1 and 2.

Starting at the origin '0' the signal turns and a lost time of duration  $L_1$  begins. Both departure curves remain horizontal until  $t = L_1$ , which locates point 'A' of the figure. At such time the signal turns green for Approach 1 and remains red for Approach 2. In this phase, denoted as Phase 1, the slopes of departure curves are  $s_1$  and 0 for movements 1 and 2 respectively. Phase 1 does not terminate when queue 1 vanishes at point 'B' of the figure. Instead, it terminates when the headway of traffic on Approach 1 is larger than the pre-determined vehicle interval (the unit extension), which is usually 2 to 5 seconds. The duration of Phase 1,  $G_1$ , is the length of segment  $AD$ . The system is now identical to that in which it was at  $t = 0$ , with the approaches reversed. Therefore, the construction of departure curve for traffic on Approach 2 is similar to what we have described for Approach 1. It goes on with a lost time  $L_2$  that causes both departure slopes to equal zero. This identifies point 'E'. The green Phase 2 begins, etc. The duration of Phase 2,  $G_2$ , is the length of segment  $EH$ .

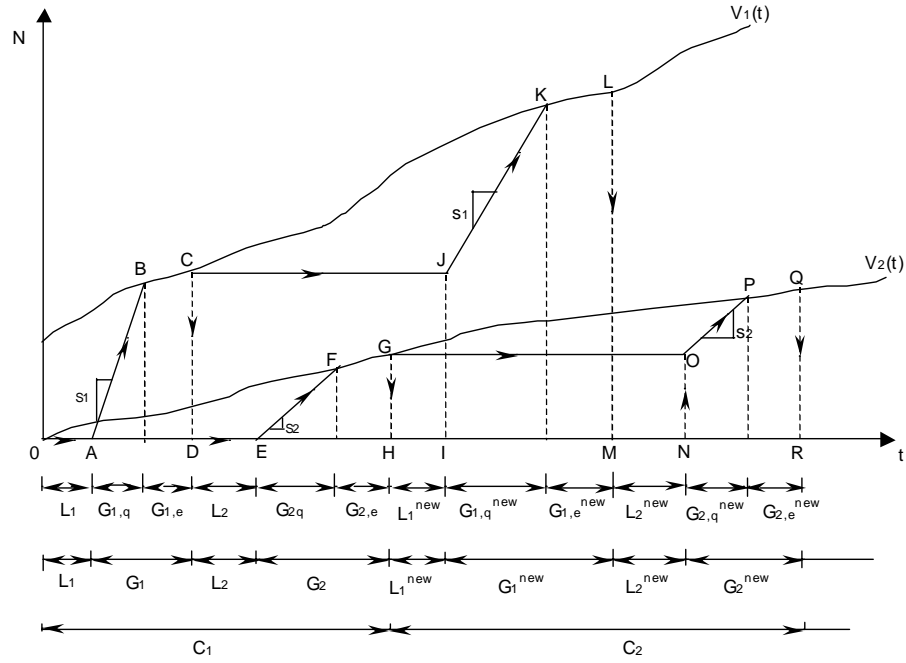


**Figure 3.4 Traffic Actuated Control Strategy**

We derive an expression for the cycle lengths and green allocations in an arbitrary cycle. Consider an arbitrary cycle  $k$ , through which the system of queues and traffic streams are observed. The cycle lasts  $C$  time units. The critical movement in Phase 1 is movement 1, while that in Phase 2 is movement 2. The green time for each phase is determined by the flow rates of movements 1 and 2 on Approaches 1 and 2, respectively. The green interval of Phase  $i$  is,  $G_i$ , for  $i = 1$  and 2. The cycle has a total lost time  $L = L_1 + L_2$ . Let  $\bar{q}_1$  denote the arrival rate of traffic on Approach  $i$  during cycle  $k$ , which is the conventional average flow rate, for  $i = 1$  and 2. By Assumptions 1 and 2, total number of arrivals on Approach 1 = total number of departures on Approach 1:

$$(G_1 + G_2 + L)\bar{q}_1 = G_{1,q}s_1 + G_{1,e}\bar{q}_1 \quad (3-12)$$

where:

$G_{1,q}$  = the queue service time during Phase 1;

$G_{1,e}$  = the green extension during Phase 1, it is a multiple of unit extension of Phase 1.

The length of the cycle is,

$$C = G_1 + G_2 + L. \quad (3-13)$$

Inserting Equation (3-13) into Equation (3-12), we have

$$C\bar{q}_1 = G_{1,q}s_1 + G_{1,e}\bar{q}_1$$

Divide both sides of the above equations by  $\bar{q}_1$ ,

$$C = G_{1,q} \frac{1}{y_1} + G_{1,e} \quad (3-14)$$

where:

$$y_1 = \bar{q}_1 / s_1. \quad (3-15)$$

When the vehicle arrival rate on Approach  $i$  for  $i = 1$  and  $2$  is high, the queue service time for vehicles from this approach also high. With high arrival rate the vehicle interarrival headway of traffic on this approach is short. Since Phase  $i$  is extended until a headway longer than the allowable gap occurs, we expect a long green extension period for this phase. Thus, the green extension is proportional to the queue service time. Let  $\alpha_1$  be the ratio of green extension period to the queue service time,

$$G_{1,e} = \alpha_1 G_{1,q}. \quad (3-16)$$

Insert Equation (3-16) into Equation (3-14),

$$G = G_{1,q} \frac{1}{y_1} + \alpha_1 G_{1,q} \quad (3-17)$$

Dividing both sides of Equation (3-17) by  $C$ , we have

$$1 = \frac{\lambda_1}{y_1} + \alpha_1 \lambda_1 \quad (3-18)$$

where:

$$\lambda_1 = G_{1,q} / C \quad (3-19)$$

Similarly, we derive the relationship between  $\lambda_2$ , and  $y_2$  for Approach 2 (See details in Appendix A).

$$1 = \frac{\lambda_2}{y_2} + \alpha_2 \lambda_2 \quad (3-20)$$

where:

$$y_2 = \bar{q}_2 / s_2 \quad (3-21)$$

$$G_{2,e} = \alpha_2 G_{2,q} \quad (3-22)$$

$$\lambda_2 = G_{2,q} / C \quad (3-23)$$

Depending on the control system,  $\alpha_i$ , may be a function of the arrival rate and distribution of traffic on approaches to the intersection. Note that  $\lambda_i$  is the ratio of queue service time ( $\bar{G}_{i,q}$ ) to the cycle length. This definition is different from that of the conventional definition where  $\lambda_i$  is the ratio of the green time to the cycle length.

### Cycle Length Expression

The cycle length equals the green times allocated to Phases 1 and 2 plus the total lost time during the cycle. For the intersection shown in Figure 3.4, the cycle length is given by Equation (3-13). The green duration for Phase  $i$  equals the time for the queue on Approach  $i$  to dissipate ( $G_{i,q}$ ), plus the green extension of Phase  $i$  ( $G_{i,e}$ ) (Refer to Figure 3.4).

$$G_1 = G_{1,q} + G_{1,e} \quad (3-24)$$

$$G_2 = G_{2,q} + G_{2,e} \quad (3-25)$$

Inserting Equations (3-24) and (3-25) into the Equation (3-13), we obtain,

$$L + (G_{1,q} + G_{1,e}) + (G_{2,q} + G_{2,e}) = C \quad (3-26)$$

Insert Equations (3-16) and (3-22) into Equation (3-26),

$$L + G_{1,q}(1 + \alpha_1) + G_{2,q}(1 + \alpha_2) = C$$

Dividing both sides of the above equation by  $C$ , and substituting  $G_{1,q}/C$  and  $G_{2,q}/C$  by  $\lambda_1$  and  $\lambda_2$ , respectively, we have

$$\frac{L}{C} + \lambda_1(1 + \alpha_1) + \lambda_2(1 + \alpha_2) = 1 \quad (3-27)$$

From Equation (3-27), we have

$$1 - \sum_i \lambda_i(1 + \alpha_i) = \frac{L}{C}$$

$$C = \frac{L}{1 - \sum_{i=1}^2 (1 + \alpha_i)\lambda_i} \quad (3-28)$$

### Expression for Green Time

Inserting Equation (3-16), (3-22) in to Equation (3-24) and (3-25) respectively, we have

$$G_1 = (1 + \alpha_1)G_{1,q} \quad (3-29)$$

$$G_2 = (1 + \alpha_2)G_{2,q} \quad (3-30)$$

From Equation (3-18), we have

$$\lambda_1 = \frac{1}{\alpha_1 + \frac{1}{y_1}} = \frac{y_1}{\alpha_1 y_1 + 1} = \frac{G_{1,q}}{C} \quad (3-31)$$

$$G_{1,q} = \frac{y_1}{\alpha_1 y_1 + 1} C$$

Insert the above equation into Equation (3-29),

$$G_1 = (1 + \alpha_1) \frac{y_1}{\alpha_1 y_1 + 1} C = \frac{y_1(1 + \alpha_1)}{1 + \alpha_1 y_1} C \quad (3-32)$$

Similarly from Equation (3-20), we have

$$\lambda_2 = \frac{1}{\alpha_2 + \frac{1}{y_2}} = \frac{y_2}{\alpha_2 y_2 + 1} = \frac{G_{2,q}}{C} \quad (3-33)$$

$$G_{2,q} = \frac{y_2}{\alpha_2 y_2 + 1} C$$

Insert the above equation into Equation (3-30),

$$G_2 = (1 + \alpha_2) \frac{y_2}{\alpha_2 y_2 + 1} C = \frac{y_2(1 + \alpha_2)}{1 + \alpha_2 y_2} C \quad (3-34)$$

The above equations for cycle length and green times can be extended to an intersection with  $n$  phases. Appendix A gives the derivation of the expressions for the cycle length and the green times with  $n$  phases, i.e., Equations (A-20) and (A-22).

#### 3.1.4 Reformulation of the Optimization Problem in terms of $\alpha_i$ and $y_i$

The cycle lengths and green times of an intersection can be expressed as functions of the parameters  $\alpha_1$  and  $\alpha_2$ . To estimate the green times and cycle length, we need to determine the parameters. The objective function of problem (3-11) can be expressed in terms of  $\alpha_i$  and  $y_i$ . We solve the optimization problem (3-11) to determine the estimated parameters and then estimate the capacity through green times and the cycle length.

The average cycle length,  $\bar{C}$ , in Equation (3-28), the uniform delay,  $d_u$ , in Equation (3-6), and the random delay,  $d_r$ , in Equation (3-10) can be expressed in terms of  $\alpha_i$  and  $y_i$ . Please refer to Appendix B for the derivation of the following expressions.

$$\bar{C} = L \frac{(\alpha_1 y_1 + 1)(\alpha_2 y_2 + 1)}{1 - (y_1 + y_2) - y_1 y_2 (\alpha_1 - \alpha_2) - \alpha_1 \alpha_2 y_1 y_2} = L \frac{(\alpha_1 y_1 + 1)(\alpha_2 y_2 + 1)}{A} \quad (3-35)$$

where:

$$A = 1 - (y_1 + y_2) - (\alpha_1 + \alpha_2) y_1 y_2 - y_1 y_2 \alpha_1 \alpha_2 \quad (3-36)$$

$$d_u = \frac{TL}{A} \left[ D_1 \frac{\alpha_2 y_2 + 1}{\alpha_1 y_1 + 1} + D_2 \frac{\alpha_1 y_1 + 1}{\alpha_2 y_2 + 1} \right] \quad (3-37)$$

where:

$$D_1 = 0.5\bar{q}_1(1 - y_1);$$

$$D_2 = 0.5\bar{q}_2(1 - y_2).$$

$$d_r = T \left[ \frac{(1 + \alpha_1 y_1)^2}{2(1 + \alpha_1)\alpha_1(1 - y_1)} + \frac{(1 + \alpha_2 y_2)^2}{2(1 + \alpha_2)\alpha_2(1 - y_2)} \right] \quad (3-38)$$

Substituting Equations (3-37) and (3-38) into the objective function of problem (3-11), we have another expression for the total delay in Problem (3-11). The optimization problem (3-11) can be presented as follows,

Minimize

$$d = \frac{TL}{A} \left[ D_1 \frac{\alpha_2 y_2 + 1}{\alpha_1 y_1 + 1} + D_2 \frac{\alpha_1 y_1 + 1}{\alpha_2 y_2 + 1} \right] + \beta T \left[ \frac{(1 + \alpha_1 y_1)^2}{2(1 + \alpha_1)\alpha_1(1 - y_1)} + \frac{(1 + \alpha_2 y_2)^2}{2(1 + \alpha_2)\alpha_2(1 - y_2)} \right] \quad (3-39)$$

Subject to: (3-11b).

The optimal parameters  $\alpha_1$  and  $\alpha_2$  can be determined by minimizing total delay in Equation (3-39). The first derivative of the objective function, Equation (3-39), has at least one root since the numerator of the derivative of the objective function is in polynomial form of  $\alpha_i$  and  $\alpha_2$ . It can be proved that the optimization problem has a unique solution. A numerical algorithm, such as Newton method, can be used to determine the optimal values of the parameters. The cycle length and the green times are determined by Equations (3-28), (3-32), and (3-34). The approach capacities are estimated by the Equation (2-15) with the estimated green times and the cycle length.

For a general case with n-phase, it is difficult to present the uniform delay in terms of  $\alpha$  values and y values. We directly calculate the cycle length and the green times from the given the  $\alpha$  values and y values. The optimization problem for determining the parameters,  $\alpha_i$ , for  $i = 1, \dots, n$  is as follows,

$$\text{Minimize } d = \frac{T}{C} \sum_{i=1}^n \left[ \frac{1}{2} \bar{q}_i (\bar{C} - \bar{G}_i)^2 \frac{1}{1 - y_i} \right] + \beta \sum_{i=1}^n \left[ \frac{\rho_i^2}{2(1 - \rho_i)} \right] T \quad (3-40a)$$

Subject to:

$$G_{i,\min} \leq \bar{G}_i \leq G_{i,\max} \text{ for } i = 1, \dots, n \quad (3-40b)$$

where:

$$C = \frac{L}{1 - \sum_{i=1}^n (1 + \alpha_i) \lambda_i} \quad (3-40c)$$

$$G_i = \frac{y_i(1 + \alpha_i)}{1 + \alpha_i y_i} C \text{ for } i = 1, \dots, n \quad (3-40d)$$

### 3.1.5 Comments on the Minimum Delay Model

In fully actuated control mode, the current phase continues showing a green indication until the actuation interval is greater than the “allowable gap.” The cycle length expressed in Equation (3-28) reflects this mechanism by letting the current phase extend a duration of  $\bar{G}_{i,e}$ . The underlying concept of fully actuated operation is that the competing demands are equally important, and that there are no arrival patterns on any approach that should be taken advantage of. The Minimum Delay Model determines the cycle length of an intersection by minimizing the overall delay at the intersection. The estimated cycle length of actuated control by this model is longer than the cycle length determined by Daganzo’s model.

The parameter  $\alpha_i$  for each critical movement is a function of flow rates and ratios of flow rate to saturation flow rate of approaches at the intersection. When  $\alpha_i$  is 0.0, the Equation (3-28) is the same as one presented by Daganzo (2000). The Equation (3-28) is a generalized model of the one presented by Daganzo (2000). Note that we do not impose any restriction on the  $V_i(t)$  curves shown in Figure 3.4. This model is appropriate for the situation when arrivals are random and/or in platoon. The cycle length estimation model, Equation (3-28), is very sensitive to the value of the total lost time,  $L$ .  $L$  must be carefully determined based on the start-up lost time and all-red time. Overestimation of  $L$  will lead to overestimating the cycle length and the capacities of approaches to an actuated intersection. System progression is often used for selection of a cycle length than isolated intersection consideration in modern traffic control, i.e., serial or network wide coordinated traffic control. However, the Minimum Delay Model does not take into account the system progression.

## 3.2 The Hybrid Model

The Hybrid Model is an improved version of capacity estimation model for actuated intersection in HCM 2000. It combines a model that estimates the queue service time and a model that estimates green extension period. We eliminate the iterative procedure that is used to determine the green times in the HCM model by computing queue service time with a deterministic queuing model.

The capacity of an approach to an actuated intersection is determined by the green time allocated to the approach and the cycle length of the intersection. In this model, queue service time and green extension period are separately estimated by two analytical models. The queue service time is estimated from the flow rates at the intersection. The green extension period is estimated based on the interarrival time distribution. The information for estimating a green time is the minimum green, the maximum green and the unit extension of the controller, the flow rate from the approach, and the length of the detector in the roadway. The green times estimated by the model are subject to the constraints of the minimum green time and the maximum green time.

*The queue service time* is estimated by the model discussed by Daganzo (2000) (see Section 2.5.2). Traffic-actuated controllers determine the queue service time for a phase

by holding the right-of-way until the accumulated queue has been served. The model determines the cycle length that corresponds to the period for queues at the intersection to dissipate. The queue service time,  $G_{i,q}$ , for phase group  $i$  can be estimated as

$$G_{i,q} = \frac{y_i}{\sum_k y_k} C_q \quad (3-41)$$

where:

$y_i$  = the ratio of the flow rate of the critical movement to the saturation flow rate for phase group  $i$ ;

$C_q$  = the proportion of the cycle length of the actuated control when all the queues vanish.

The  $C_q$  is estimated by Equation (2-25). We restate it here,

$$C_q = L \left( 1 - \sum_k y_k \right)^{-1} \quad (3-42)$$

To account for randomness in arrivals, we multiply the green time estimated by Equation (3-42) by a factor  $f_q$  proposed by Akcelik (1993). The adjusted queue service time is,

$$G_{i,q} = f_{q,i} \frac{y_i}{\sum_k y_k} C_q \quad (3-43)$$

where

$$f_{q,i} = 1.08 - 0.1(G_{a,i} / G_{\max,i})^2$$

$G_{a,i}$  = the actual green for phase group  $i$ , seconds;

$G_{\max,i}$  = maximum green for phase group  $i$ , seconds.

The actual green time for each phase group is obtained as

$$G_{a,i} = G_{ef,i} + l_i - \tau_i \quad (3-44)$$

where  $\tau_i$  is yellow time for phase group  $i$ .

*The green extension period* is the expected waiting time for a gap longer than “allowable gap” to occur, given that the probability distribution of the vehicle headway is bunched negative exponential (Akcelik, 1994). The green extension period depends on the approach flow rate, the detector design parameters in the approach, and the settings of the controller. The green extension period of phase group  $i$  is estimated by the model reviewed in Section 2.5.3. We restate them here,

$$G_{i,e} = \frac{e^{\theta(e_0 + t_0 - \Delta)}}{\phi q} - \frac{1}{\theta}, \quad (3-45)$$

$$t_0 = 0.68(L_d + L_v) / S_A, \quad (3-46)$$

$$\theta = \frac{\varphi q}{1 - \Delta q}, \quad (3-47)$$

$$\varphi = e^{-b\Delta q}, \quad (3-48)$$

where the definitions of the variables and the recommended parameter values are in Section 2.5.3.

After the queue service time and the green extension period are estimated by the above models, i.e., Equations (3-43) and (3-45), the effective green time for each phase group  $i$  is given by:

$$G_{ef,i} = G_{i,q} + G_{i,e}. \quad (3-49)$$

The cycle length of the intersection is the sum of effective green times allocated to each phase group. The cycle length is given by:

$$C = \sum_i (G_{ef,i} + l_i) \quad (3-50)$$

where  $l_i$  is lost time for phase group  $i$ .

The capacity of a lane group can be determined by Equation (2-15) after the green times and the cycle length have been determined. The Hybrid Model is sensitive to the value of the total lost time,  $L$ , because the queue service time is function of the total lost time. This model is also sensitive to the value of unit extension, because the green extension time is determined based on the vehicle interarrival time distribution and the green extension terminates when the vehicle headway is longer than the “allowable gap,” which is usually the unit extension.

### 3.3 Treatment of Left-turn flow Rates in Capacity Estimation

On a permitted left-turn phase, left-turning vehicles execute their turning maneuvers through gaps in the opposing traffic stream. The first gap, however, does not appear until the queue of opposing vehicles clears the intersection. If a left-turner arrives during the interval in which the opposing queue is clearing, it effectively blocks the lane for both through and left-turning vehicles (assuming left-turn and through traffic uses a shared lane) until the first gap appears. Any lane blockages or congestion in the shared lane will influence traffic lane distribution as vehicles move to adjacent lanes to avoid turbulence and delays. If a through vehicle arrives at the intersection at the time that a gap appears in the opposing traffic stream, no left-turning vehicle will be able to use the gap. A large number of through vehicles in the shared lane may block so many of the available gaps as a result of insufficient capacity left for left-turning vehicles.

As a result, the approach capacity is not sufficiently used by the left-turners under permitted left-turn phasing. We need to adjust the left-turn volume to account for the fact that the left-turners need more time to pass through the intersection and they also block

the through-vehicles on their approach. Mcshane (1990) discussed an approach for converting left-turn flow rate to an approximate equivalent flow rate of through vehicle when determining whether an approach may be used by both left-turning vehicles and through vehicles. The conversion formulas is:

$$v_{LE} = v_L \times \frac{1}{1400/1800 - v_o / s} \quad (3-51)$$

where:

$v_{LE}$  = approximate equivalent left-turn flow rate (vph),

$v_L$  = actual left-turn flow rate (vph),

$v_o$  = total opposing through flow rate (vph),

$s$  = saturation flow rate (vph).

The left-turn flow rate can be converted to an approximate equivalent flow of through vehicles by Equation (3-51). Note that when  $v_o/s$  equals or is greater than (1400/1800) vph,  $v_{LE}$  has no meaning. In such case, left-turn movement against the opposing flow is not possible.

Under extreme conditions, the equivalent left-turn flow,  $v_{LE}$ , completely occupies the leftmost lane of the approach. The remaining flow uses the remaining lanes equally. If the equivalent left-turn flow rate is less than the average flow rate in the remaining lanes, some through vehicles will share the left-turn lane. We do not distinguish these two cases since all the movements on the approach are shown green indication simultaneously. We just need to add the equivalent left-turn flow rate to the through traffic volume when we use the Minimum Delay Model or the Hybrid Model estimating the green times and cycle lengths.

When left-turn vehicles move separately from an opposing through traffic (e.g., with “protected” phasing), the time dedicated to this movement is not available for the through movement. When an exclusive bay or lane is used, i.e., the left-turn phase is protected, some or all left turn vehicles move on a protected phase. There is no interruption between the left-turn traffic and the opposing through traffic. The cycle lengths and green times are computed as multi-phases with longer lost time since additional “lost time” generally occurs.

## Chapter 4 Implementation of Capacity Estimation Models in DynaMIT

### 4.1 Introduction to DynaMIT

Dynamic Network Assignment for the Management of Information to Travelers (DynaMIT) utilizes various models and algorithms to estimate network state and predict route guidance information. The overall structure with interactions among the various elements of DynaMIT is illustrated in Figure 4.1.

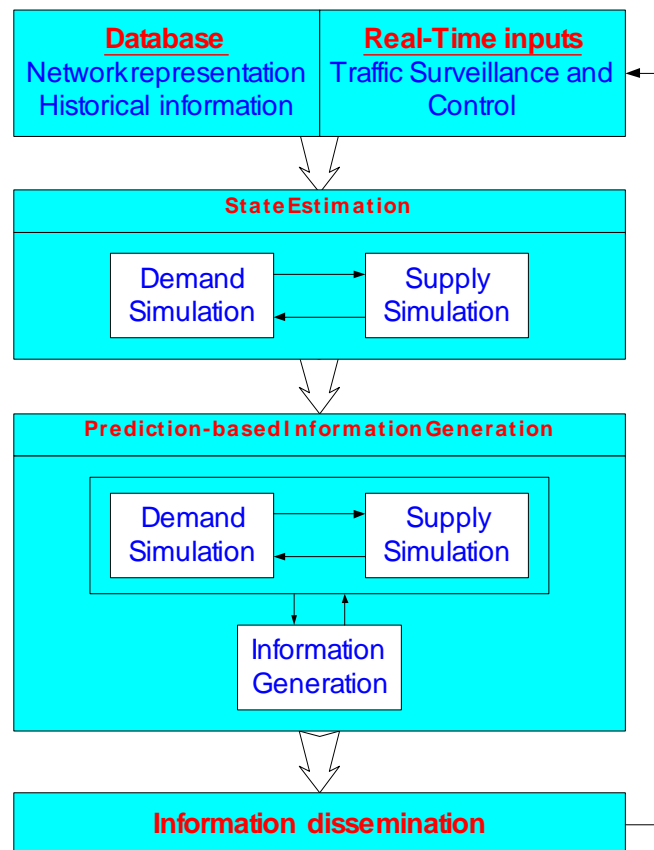


**Figure 4.1 Structure of DynaMIT**

DynaMIT utilizes both off-line and real-time information. The off-line information includes: the detailed description of the network and historical network conditions. The historical database contains time-dependent data such as origin-destination matrices and link travel times. The real-time information is provided by the surveillance system and the control system. DynaMIT is designed to operate with a wide range of surveillance and control systems, which provide real-time link flows, incident characteristics, and traffic control strategies. The network state estimator utilizes a mesoscopic traffic simulation model, which simulates the actual traffic conditions in the network starting from the beginning of the previous time period to the present time. Inputs include

demand, updated capacities and traffic dynamics parameters, and control strategies implemented.

Mesoscopic Traffic Simulator for DynaMIT simulates the movement of vehicles on the network for the given supply simulation interval. The simulation starts at time zero which is the beginning of the simulation interval. There are a simulation interval, an update interval, and an advanced interval. The simulation interval is the entire time that the supply module runs. For each simulation interval there are a number of update intervals, which are used to report information of link flows, queues and densities. For each update interval there are one or more advance intervals, during which traffic is moved. Figure 4.2 shows simulation process along with various time intervals.

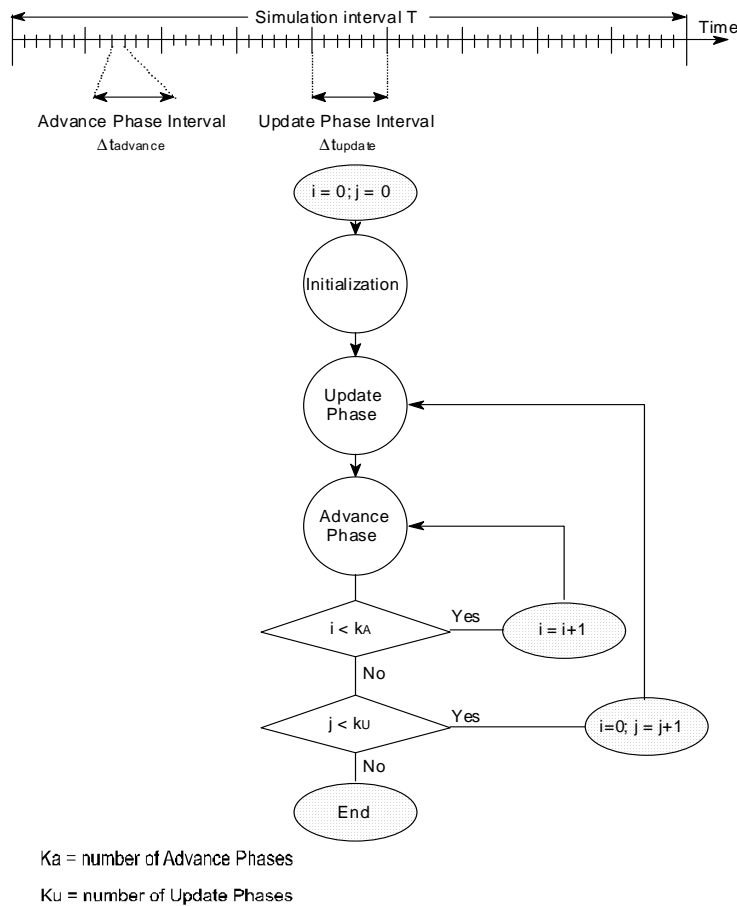


**Figure 4.2 Simulation Process**

The network representation consists of static and dynamic components. The static components represent the topology of the network. The dynamic components capture the traffic dynamics, which are continuously updated. Each link of the road network is divided into segments that capture variations of traffic conditions along the link. Traffic dynamics within a segment are captured by lane groups and directions. Each

segment/lane group has a capacity constraint at the downstream end. The capacity of a segment is represented as acceptance capacity, which is the number of vehicles that can potentially join the segment. The output capacity of a lane group at an intersection is a function of the saturation flow, the effective green time, and the cycle time.

The ATMS component is the interface between DynaMIT and the Advance Traffic Management System. Its role is to transform the control logic of each device into capacities of road segments or lane groups, which are used by the Traffic Simulator. The structure of the mesoscopic traffic simulator is shown in Figure 4.2. The traffic characteristics parameters and capacities of segments/lane groups are updated in “Update Traffic” component. The proposed capacity estimation models for actuated intersections are implemented in the traffic simulator of DynaMIT to dynamically estimate the segment/lane group capacities. The capacities are updated in a capacity update interval, which has one or several update intervals. In this chapter capacities are referred to lane groups. All the methods discussed can be directly applied to capacities of approaches to the intersections.

#### **4.2 Implementation of the Minimum Delay Model and the Hybrid Model**

We estimate the capacity of lane groups at an intersection by the Minimum Delay Model or the Hybrid Model in DynaMIT. The Minimum Delay model only needs the flow rates of lane groups to estimate the capacities at an actuated intersection. The Hybrid Model requires more input data than the Minimum Delay Model, but it is faster than the other model. Green times and cycle lengths are estimated using the proposed models, and lane group capacities are computed by Equation (2-15) in every capacity update interval in DynaMIT.

To estimate the capacity of lane groups, we need to determine the parameters of the Minimum Delay Model. For intersections with two phases, we compute the cycle length and green times using Equations (3-28), (3-32), and (3-34). For  $n$  phase case, we use Equations (A-20) and (A-22) described in Appendix A to compute the green times and cycle lengths. We solve the optimization problem (3-40) by a numerical algorithm to determine the parameters. Although traffic demand varies from time to time, there should not be significant variations in traffic demand in a short period. Therefore, we can reasonably assume that the parameters do not change in a short interval, e.g., a simulation interval in DynaMIT. Thus, we only estimate the parameters in every simulation interval. The parameters are estimated using traffic volumes in the previous simulation interval for the first iteration of a simulation interval and using traffic volumes in the previous iteration for the second and the following iterations of the same simulation interval. Although we need to evaluate the objective function, the total delay, at every iteration to determine the optimal parameters, the optimization problem (3-40) can still be implemented efficiently by choosing an efficient numerical algorithm.

#### 4.2.1 Averaging the Lane Group Capacities

The parameters at iteration  $k$ ,  $\alpha_k$ , are used to compute capacities of lane groups in every capacity update interval in DynaMIT. Ideally, we should use current traffic volumes to estimate the capacity of lane groups at an intersection in dynamic traffic assignment. However, the simulated traffic volumes depend on the capacities of lane groups at the intersections since the solution to the traffic assignment is subject to the constraints of intersection capacities. Therefore, an iterative process should be used to determine the capacities. Since we use an iterative procedure to solve dynamic traffic assignment in DynaMIT, we can estimate the capacities in the same iterative procedure. Since traffic evolves smoothly from a short time interval  $t$  to another short time interval  $t+I$  (the length of the time interval is usually capacity update interval in DynaMIT), the flow rates in time interval  $t$  are approximately the same as those in time interval  $t+I$ . The capacities estimated using the flow rates in interval  $t$  can approximate the capacities in interval  $t+I$ . However, we average the capacities determined using the flow rates in time interval  $t$  and the averaged values used in the interval,  $t$ , to approximate the capacities of lane groups used in interval  $t+I$  traffic assignment.

Let  $c_a^t$  be the averaged capacity of lane group  $a$  used in the time interval  $t$  and  $\hat{c}_a^t$  be capacity calculated based on the simulated flow rates in the current interval  $t$ . The weighted average of the lane group capacities for traffic assignment in time interval  $t+I$  is computed by

$$c_a^{t+1} = \gamma c_a^t + (1 - \gamma) \hat{c}_a^t \quad (4-1)$$

where  $\gamma$  is the weight factor,  $\gamma \in [0, 1]$ .

We can also average the green times, and then compute the capacity from the green times and the cycle lengths. Let  $G_a^t$  be the weighted effective green time used in time interval  $t$  for lane group  $a$ ; let  $\hat{G}_a^t$  be effective green duration computed using the simulated flow rates in the current time interval,  $t$ . We average the above two values of green indication durations and use the averaged green time to estimate the capacity of the lane group that is used for traffic assignment in time interval  $t+I$ ,

$$G_a^{t+1} = \gamma G_a^t + (1 - \gamma) \hat{G}_a^t \quad (4-2)$$

where  $\gamma$  is the weight factor,  $\gamma \in [0, 1]$ .

The cycle length of intersection  $n$  for computing the lane group capacity in interval  $t+I$ ,  $C_n^{t+1}$ , is calculated as,

$$C_n^{t+1} = \sum_{a \in \text{intersection } n} G_a^{t+1}. \quad (4-3)$$

The capacities are computed by Equation (2-15) using the average green times and cycle lengths.

#### 4.2.2 Input Data for the Capacity Estimation Models

To determine the lane group capacities of an actuated intersection, the Minimum Delay Model and the Hybrid Model require the phase configuration, the minimum green time and the maximum green time for each phase, the saturation flow rate of each lane group, and the speed limit of each approach. The Hybrid Model also requires the unit extension as input. See input format of these data in Appendix C.

### 4.3 Imposing Lower Bound on Green Times and Initial Lane Group Capacities

In traffic assignment with actuated traffic control, any assignment of zero flow on a lane group will result in allocation of zero green time to that lane group. In turn, the green time allocated to that lane group would remain zero in all following time intervals because of the capacity used is zero. Obviously, such estimation is not realistic because the lane group at an intersection must always be provided some period of green indication for safety reasons. Lower bounds on green times should be imposed to meet the technical requirements and to produce realistic results.

In the first update interval in the first simulation interval in DynaMIT, there is not traffic on the network. The capacities of lane group at actuated intersections are estimated by the maximum green times. After substantial vehicles are loaded onto the network, e.g., after the first update interval in the first simulation period, lane group capacities are estimated using the simulated traffic volumes. Lane group capacities in the first update interval of a simulation interval other than the first simulation interval are computed based on the accumulated flows in the previous simulation interval because flows of the last capacity update interval are more random than aggregated flows in the simulation interval.

## Chapter 5 Validation of the Proposed Models

The proposed models are validated at both the intersection level and the network level. At the intersection level, two isolated intersections with actuated control are simulated in detail in MITSIM-Lab. The estimation results from the two proposed models are compared with simulation results from MITSIM-Lab. At the network level, a real network from Irvine, CA is used for validating the capacity estimation models. The traffic volumes, simulated by DynaMIT with capacity estimated by the proposed models at intersections with actuated control, are compared with the field observations to test the performance of the proposed models.

### 5.1 Validation of the Proposed Models at Intersection Level

We compare the estimation of green times by the proposed models with those simulated by MITSIM-Lab because we do not have minute-by-minute signal timing data of real-life operations. The operations of two intersections in Irvine, CA are simulated by MITSIM-Lab with the real controller settings. We also compare the green times and cycle lengths estimated by the proposed models -- the Minimum Delay and the Hybrid -- with Webster's model and the model for actuated control from the TSC Handbook (1996).

#### 5.1.1 Introduction to the Two Intersections

The intersection of Irvine Center Drive and Laguna Canyon has eight phases. The intersection layout and vehicle movements are shown in Figure 5.1. Irvine Center Dr. is an arterial road with the speed limit of 55 mph. The speed limit of Laguna Canyon is 45 mph. The signal control is a fully actuated NEMA controller. Phases 1, 5, 3, and 7 are protected left-turn phases. Phase sequences and signal timing plans are also shown in Figure 5.1.

The intersection of Laguna Canyon and Pasteur has six phases. The layout of the intersection and vehicle movements is shown in Figure 5.2. The speed limit of Laguna Canyon is 45 mph, while that of Pasteur is 35 mph. The signal control is a fully actuated NEMA controller. Phases 1, 5, 2, and 6 are protected phases. The Eastbound left-turn on Pasteur, a secondary road, and the Westbound left-turn are permitted phrases. Vehicles, making the above two left-turns, move together with the corresponding through traffic. Phase sequences and signal timing plans are also shown in Figure 5.2.

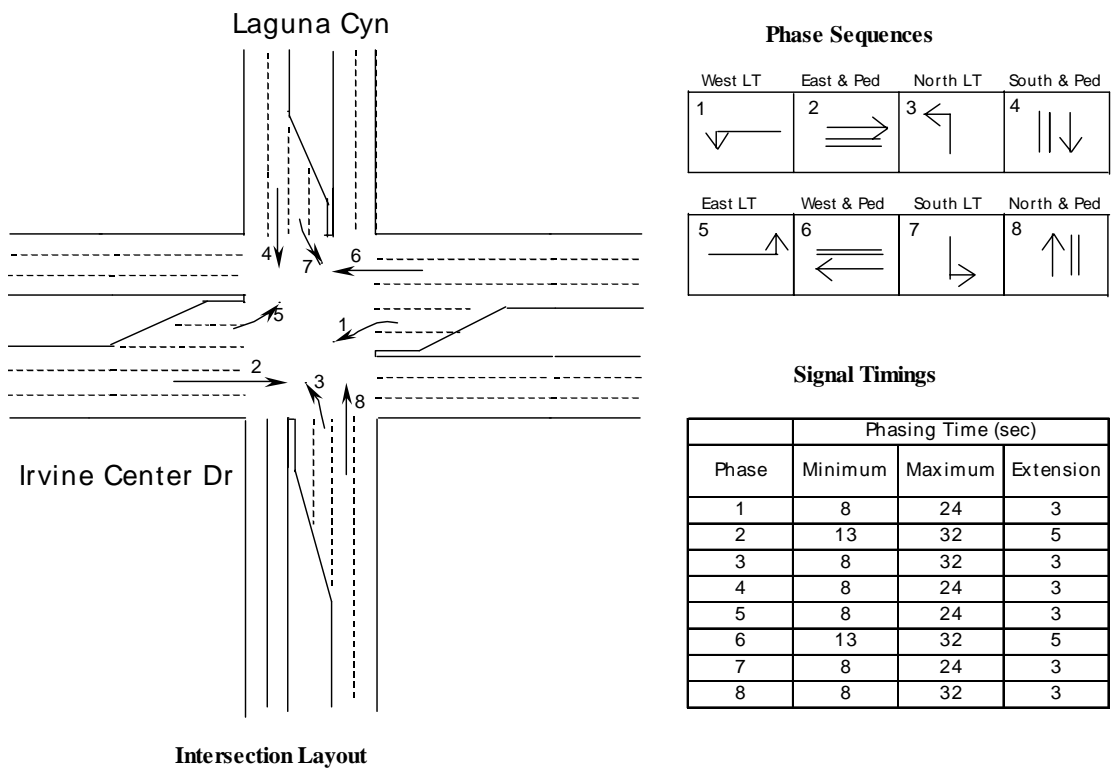


Figure 5.1 Intersection of Irvine Center Dr and Laguna Cyn (Protected Phasing)

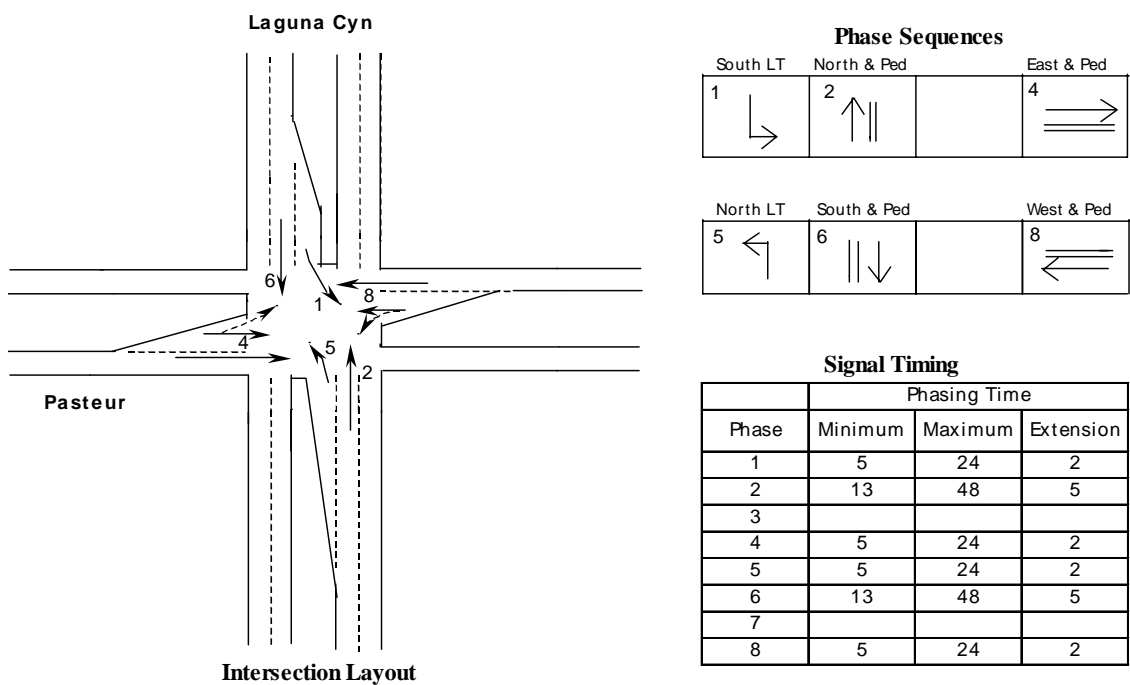


Figure 5.2 Intersection of Pasteur @ Laguna Cyn with One Permitted Left Turn Phase

### Saturation flow rate at the intersection of Irvine Center Dr. and Laguna Canyon

The “ideal” saturation flow rate,  $s_0$ , is 1900 passenger cars per hour of green time per lane (pcphgp). The value is adjusted for a variety of prevailing conditions that are not ideal. The HCM 2000 suggests up to eleven adjustment factors for the modification of the ideal saturation flow rate. We consider three of them, which are applicable to this intersection: Lane width, Area type, and Left turn. The *Lane-width factor*,  $f_w$ , represents the impact of lanes wider than the defined “ideal” 12-ft lane on saturation flow rate. Since both Irvine Center Dr. and Laguna Canyon have speed limits above or equal to 45 mph, we can reasonably think that the lane width of each road is greater than 12 ft. The factor for lane-width is 1.067 according to HCM 2000. The *area-type factor*,  $f_a$ , is 1.0 since the intersection is not in Central Business District (CBD). The *left-turn factor*,  $f_{LT}$ , is 0.95. The left-turn adjustment factor is based on factors including, the left turns are made from exclusive lanes and the type left-turn phase is protected. The value is chosen based on the above factors according to HCM 2000. Irvine Center Dr. is a three-lane road and expands to five lanes close to the intersection. Laguna Canyon is a two-lane arterial road and expands to four lanes close to the intersection. Because of the constraints of the upstream streets, the lanes close to the intersection are not fully used. We apply an adjustment factor, 0.90, to the saturation flow rates to the lane groups of this intersection. The saturation flow rate for each lane group is shown in Table 5-1.

**Table 5-1 Saturation Flow Rates (vphg)**

Movement	Orientation	$s_0$	Adjustment Factor	Number of Lanes	s
1	West LT	1900	0.855	2	3249
5	East LT	1900	0.855	2	3249
2	East Thr	1900	0.960	3	5474
6	West Thr	1900	0.960	3	5474
3	North LT	1900	0.855	2	3249
7	Sourth LT	1900	0.855	2	3249
4	Sourth Thr	1900	0.960	2	3649
8	North Thr	1900	0.960	2	3649

Note:

s = saturation flow rate for the subject lane group, expressed as a total for all lanes in the lane group under prevailing conditions, in vphg.

### Saturation flow rate at the intersection of Laguna Canyon and Pasteur

The “ideal” saturation flow rate is 1900 pcphgp. The value is adjusted for lane width, area type, and left turn. The factor for lane-width is 1.067 according to HCM 2000. The area-type factor,  $f_a$ , is 1.0 since the intersection is not in CBD. The left-turn factor,  $f_{LT}$ , is chosen based on whether the left-turns are made from exclusive lanes according to HCM 2000. For the protected left-turn lane groups, the adjustment factor is 0.95. A special computation is needed to adjust the saturation flow rates for the approaches, which have permitted left-turn phasing. We simply assume the adjustment factor for the lane group

used by both left-turn and through vehicles is 1.0 and that for the through traffic is 1.067. The saturation flow rate for each lane group is shown in Table 5-2.

**Table 5-2 Saturation Flow Rates (vphg)**

Movement	Orientation	$s_0$	Adjustment Factor	Number of lanes	$s^1$
1	South LT	1900	0.95	1	1805
5	North LT	1900	0.95	1	1805
2	North Thr	1900	1.067	2	4055
6	South Thr	1900	1.067	2	4055
4	East LT, Thr <sup>2</sup>	1900	1.067	2	3927
8	West LT, Thr <sup>2</sup>	1900	1.067	2	3927

Note:

1.  $s$  = saturation flow rate for the subject lane group, which is the total for all lanes in the lane group under prevailing conditions, in vphg
2. The saturation flow rate =  $1.067 \cdot 1900 + 1900$  pcphg.

#### 5.1.2 Comparison of the Proposed Models with those from TCS Handbook

In this section, we give a numerical comparison of the Minimum Delay Model and the Hybrid Model with Webster's and the TCS Handbook model for actuated control shown in Equation (2-33). The Minimum Delay Model minimizes the total delay of critical movements (which have a higher ratio of flow to saturation flow in their phase group). The Hybrid Model determines the green times by a M/G/1 queuing model and the headway probability distribution. The two models are distinguished from the Webster's model and the TCS Handbook model by the way they determining the green time for each phase group.

We use the intersection of Irvine Center Dr. and Laguna Canyon to compare the Minimum Delay Model and the Hybrid Model with Webster's model and the TCS Handbook model for actuated control. The traffic volumes on Lane Groups 1 and 5, 2 and 6, 3 and 7, and 4 and 8 are the same. The demands on the Lane Groups 1, 2, 3, and 4 increase proportionally from 338 vph, 912 vph, 338 vph, and 608 vph, to 525 vph, 1418 vph, 525 vph, and 946 vph respectively. The lost time is 4 seconds per phase and all-red time is 1 second at this intersection. The green times and cycle lengths for each level of traffic volumes are shown in Table 5-3.

The estimated cycle lengths from the Minimum Delay Model are between the estimations by the TCS Handbook model for actuated control and those by Webster's when the sum of flow ratios of critical movements is between 0.70 and 0.80. The estimations from the Minimum Delay Model are roughly 2 to 30 percent higher than those by the TCS Handbook model and are about 2 to 30 percent lower than those from Webster's. The Minimum Delay Model estimates longer cycle than Webster's when the sum of flow ratios of the critical movements is below 0.7 and it estimates shorter cycles than Webster's if the sum of flow ratios of the critical movements is above 0.7.

The estimations of cycle lengths by the Hybrid Model are between the estimations by the TCS Handbook model and those by Webster's when the sum of flow ratios of critical movements is between 0.70 and 0.80. The estimated cycle lengths from the Hybrid Model are lower than those estimated by the Webster's model and when the sum of flow ratios of the critical movements is above 0.7. The cycle lengths estimated by the Hybrid Model are higher than those estimated by the Webster's and the TCS Handbook model when the sum of flow ratios is below 0.7.

**Table 5-3 Comparison of Timing Plans Estimated by Four Different Models**

Flow Rate on Lane Group (vph)					Sum of Critical Flow Ratios <sup>1</sup>	TCS Handbook Model for actuated control					Webster's Model				
						Effective Green Time on Lane Group (sec)				Cycle length (sec)	Effective Green Time on Lane Group (sec)				Cycle length (sec)
1	2	3	4		1 & 5	2 & 6	3 & 7	4 & 8		1 & 5	2 & 6	3 & 7	4 & 8		
525	1418	525	946	0.757	22	35	22	35	135	31	50	31	50	181	
488	1317	488	878	0.703	16	26	16	26	104	23	37	23	37	140	
450	1216	450	811	0.649	12	20	12	20	84	18	29	18	29	113	
413	1114	413	743	0.595	10	16	10	16	71	15	23	15	23	96	
375	1013	375	676	0.541	8	13	8	13	61	12	19	12	19	83	
338	912	338	608	0.487	7	10	7	10	54	10	16	10	16	73	
263	709	263	473	0.379	5	7	5	7	44	7	12	7	12	59	
188	507	188	338	0.270	3	5	3	5	37	6	9	6	9	49	
113	304	113	203	0.162	2	4	2	4	31	4	7	4	7	42	
Flow Rate on Lane Group (vph)					Sum of Critical Flow Ratios <sup>1</sup>	Minimum Delay Model					Hybrid Model				
						Effective Green Time on Lane Group (sec)				Cycle length (sec)	Effective Green Time on Lane Group (sec)				Cycle length (sec)
1	2	3	4		1 & 5	2 & 6	3 & 7	4 & 8		1 & 5	2 & 6	3 & 7	4 & 8		
525	1418	525	946	0.757	24	32	24	32	132	24	32	24	32	132	
488	1317	488	878	0.703	21	32	21	32	126	20	32	20	32	124	
450	1216	450	811	0.649	19	32	19	32	121	17	32	17	28	114	
413	1114	413	743	0.595	15	26	15	24	100	16	25	16	25	101	
375	1013	375	676	0.541	14	24	14	21	93	16	22	16	22	95	
338	912	338	608	0.487	14	24	14	18	90	16	20	16	21	92	
263	709	263	473	0.379	11	18	11	11	71	12	18	13	17	80	
188	507	188	338	0.270	11	18	11	11	71	12	17	12	16	77	
113	304	113	203	0.162	11	18	11	11	71	12	15	12	15	74	

Note:

1. Sum of Critical Flow Ratios = sum of  $q_i/s_i$  for critical movement  $i$ ,  $i = 1, \dots, 8$ .

The TCS Handbook model for actuated control underestimates the cycle length. For example, when the demands on Lane Groups 1, 2, 3, and 4 are 488 vph, 1317 vph, 488 vph, and 878 vph respectively, the green times for two phase groups of through movements should be the maximum green times and the cycle length should be close to the maximum cycle length. If we use TSC Handbook model, the estimated cycle length is only 104 seconds. At this level of demand, the capacity of lane groups 1, 2, 3 and 4 are  $(15.8/104) \times 3429 = 520$  vph, and  $(26.6/104) \times 5474 = 1404$  vph,  $(15.8/104) \times 3429 = 520$  vph, and  $(25.4/104) \times 3649 = 894$  vph, respectively. Because traffic arrivals are random,

some cycles may fail in serving the queues on some lane groups with high  $v/c$  ratio such as lane groups 4 and 8 with flow ratio being 0.98. This will result in longer delay on lane groups 4 and 8. Furthermore, shorter cycle length also increases total lost time during a cycle. Therefore, at this level of demand, the controller operates with the maximum greens for phases 2, 6, 4, and 4. Then, the TCS Handbook model is not applicable to the estimation of lane group capacities in dynamic traffic assignment.

In contrast, the estimation of cycle length from the Minimum Delay Model is 126 seconds, which is longer than that from TCS Handbook model for the same intersection with the same level of demand. The capacity of Lane Groups 1, 2, 3 and 4 are  $(21/126) \times 3429 = 575$  vph, and  $(32/126) \times 5474 = 1418$  vph,  $(21/126) \times 3429 = 575$  vph, and  $(32/126) \times 3649 = 924$  vph, respectively. The  $v/c$  ratios for Lane Groups 1,2,3 and 4 are 0.85, 0.93, 0.85, and 0.95, respectively. The cycle length estimation from the Hybrid Model is 124 seconds, which is longer than that from TCS Handbook model. The capacity of Lane groups 1, 2, 3, and 4 are  $(20/124) \times 3429 = 544$  vph, and  $(32/124) \times 5474 = 1418$  vph,  $(20/124) \times 3429 = 544$  vph, and  $(32/124) \times 3649 = 945$  vph, respectively. All the lane groups have enough capacities for traffic to go through the intersection.

The Minimum Delay Model and the Hybrid Model estimates longer cycle lengths than the TCS Handbook model when intersections are not saturated. The capacities estimated by the two proposed models are larger than the traffic demands. Thus, the Minimum Delay Model and the Hybrid Model are more applicable to the DTA than the TCS Handbook model.

### 5.1.3 Comparison of the Green Times Estimated by Proposed Models with those simulated by MITSIM-Lab at An Intersection with Eight Protected Phases

The allocation of green times is an important input of the estimation of lane group capacity. The Minimum Delay Model and the Hybrid Model determines the capacity of a lane group of the intersection by estimating the cycle length of an intersection and effective green times for each lane group. The most desirable way to test the performance of the proposed models is to compare the green times and the cycle length estimated by the Minimum Delay Model or the Hybrid Model with actual minute-by-minute observations. However, this comparison is not possible because these data are not available. MITSIM-Lab simulates the controller such NEMA based on control parameters and logic for signal operation read from input file. We use MITSIM-Lab to simulate operation of the signal at the intersection of Irvine Center Dr. and Laguna Canyon in Irvine, CA with different levels of traffic volumes. We compare the green time estimations from the proposed models with those from MITSIM-Lab simulation at this intersection.

### Comparison Criteria

Our objective is to estimate capacity of lane groups of an intersection for dynamic traffic assignment. We can record the MITSIM-Lab output flow rate of each lane group of the intersection and then compare the simulation results with the capacities estimated by the

proposed models. However, this comparison is not useful because the output flow rate of a lane group simulated in MITSIM-Lab does not equal the lane group capacity, which is estimated by the Minimum Delay Model or the Hybrid Model.

Consider an approach to the intersection, for example Approach 1, which is unsaturated, shown in Figure 3.4. The figure shows the arrival and departure curves of vehicles on this approach. Queues build up during the red time and dissipate completely during the green time, i.e., the approach is not saturated. During period  $G_{1,q}$ , which is a part of green time, the vehicle dissipation rate equals the saturation flow rate. The dissipation rate equals the arrival rate during the period  $G_{1,e}$  that is the other part of the green time during which approaching vehicles do not stop. The output volume is  $(s_1 G_{1,q} + q_1 G_{1,e}) / C_1 < s_1 (G_1 / C_1)$  where  $G_1$  is the total effective green time allocated to Approach 1. If we repeat the experiment for one hour, we get the average output flow rate by averaging output volume of all the cycles in the hour. The output flow rate is  $(s_1 \bar{G}_{1,q} + q_1 \bar{G}_{1,e}) / \bar{C} < s_1 (\bar{G}_1 / \bar{C})$  where  $\bar{G}_{1,q}$ ,  $\bar{G}_{1,e}$ ,  $\bar{G}$ ,  $\bar{C}$  are the average queue service time, average green extension period, effective green time, and the average cycle length. Therefore, the capacity of an approach is larger than output volume simulated by MITSIM-Lab if the intersection is under saturated. If the intersection is saturated, the output flow rate equals  $s_a (\bar{G} / \bar{C})_a$  which is the capacity of this approach. The capacity of an approach estimated by the Minimum Delay Model should equal the output flow rate simulated by MITSIM-Lab. Therefore, we should compare the ratios of the effective green time to the cycle length, and average cycle length simulated by MITSIM-Lab with those estimated by the proposed models.

### Adjustment of Flow Rate

When Right Turn on Red (RTOR) is permitted, the right-turn movements are “shadowed” by the protected left-turn phases from the cross street. For example, the westbound left-turn (on Irvine Center Dr.) will shadow the northbound right turn (on Laguna Canyon). Free-flowing right turn volumes that are not under signal control are removed from the analysis. When we simulate the vehicle movement in MITSIM-Lab, we send 338 vehicles per hour on each right-turn lane. Since some vehicles are not under the signal control, we remove 50 percent of the right turn vehicles from the input flow of each right-turn movement.

### Testing Scenarios

The comparison of the estimations of effective green ratios estimated by the Minimum Delay Model or the Hybrid Model with those simulated by MITSIM-Lab is conducted with three testing scenarios, i.e., heavy, normal, and light traffic volumes. These three scenarios are listed in Table 5-4.

**Table 5-4 Flow Rates into the Intersection**

Movement	Orientation	Traffic Volume Scenarios (vph)		
		Heavy	Normal	Light
1	West LT	750	450	338
5	East LT	750	450	338
2	East Thr	2026	1216	912
6	West Thr	2026	1216	912
3	North LT	750	450	338
7	Sourth LT	750	450	338
4	Sourth Thr	1351	811	608
8	North Thr	1351	811	608

Note:

The adjusted flow rate of through movement = flow rate of through movement  
+ 0.5\*flow rate of right-turn movement

### Comparison of Effective Green Ratios for Lane Groups

The green ratios estimated by the Minimum Delay Model and the Hybrid Model, and the simulated by MITSIM-Lab are presented in Table 5-5. The comparison of green ratio estimated by the three models under different scenarios is represented as bar charts shown in Figure 5.3 to Figure 5.5.

**Table 5-5 Effective Green Ratios Estimated by Different Models under Different Scenarios at Intersection of Irvine Center Dr and Laguna Cyn**

Movement	Orientation	Heavy			Normal			Light		
		MITSIM	Minimum Delay	Hybrid	MITSIM	Minimum Delay	Hybrid	MITSIM	Minimum Delay	Hybrid
1	West LT	0.182	0.194	0.182	0.154	0.155	0.147	0.129	0.117	0.151
5	East LT	0.179	0.194	0.182	0.151	0.155	0.147	0.132	0.117	0.151
2	East Thr	0.252	0.258	0.242	0.281	0.264	0.282	0.329	0.198	0.309
6	West Thr	0.254	0.258	0.242	0.284	0.264	0.282	0.326	0.198	0.309
3	North LT	0.186	0.194	0.182	0.159	0.155	0.150	0.138	0.117	0.153
7	Sourth LT	0.184	0.194	0.182	0.162	0.155	0.150	0.129	0.117	0.153
4	Sourth Thr	0.249	0.258	0.242	0.261	0.260	0.246	0.233	0.147	0.194
8	North Thr	0.249	0.258	0.242	0.261	0.260	0.246	0.241	0.147	0.194
Cycle length (sec)		130	132	132	121	121	114	103	90	104
Total Simulation time (sec)		3560	3600	3600	3559	3600	3600	3565	3600	3600

Note: The green times and green ratios are average values of four runs.

The actuated signal operates at maximum green time with heavy demand simulated by MITSIM-Lab as shown in Table 5-5 and Figure 5.3. The green times and cycle length simulated by MITSIM-Lab are the same as those estimated by the Minimum Delay Model and the Hybrid Model.

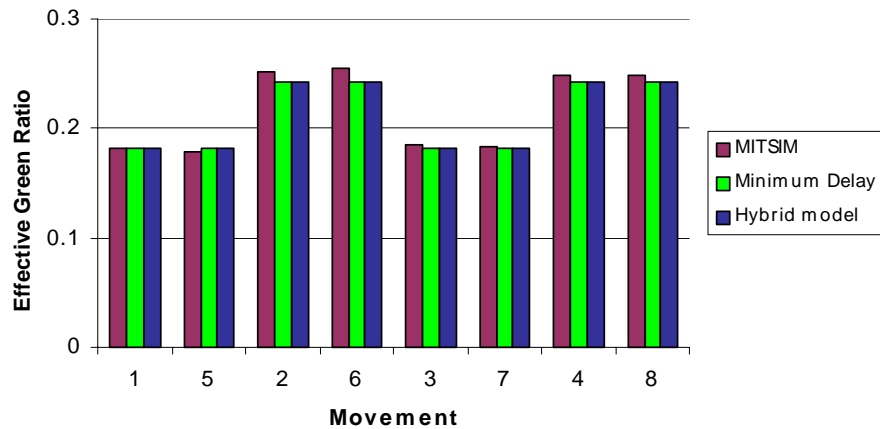


**Figure 5.3 Heavy Traffic Volume**

The green ratios for movements 1, 5, 3, 7, 4, and 8 simulated by MITSIM-Lab are approximately the same as those estimated by the Minimum Delay Model with normal demand (shown in Table 5-5 and Figure 5.4). The sum of ratios of flow rate to the saturation flow rate for the critical movements is 0.70 for this case. The green ratios for movements 2 and 6 simulated by MITSIM-Lab are higher than those estimated by the Minimum Delay Model. This difference can be explained by the equal saturation principle used by the Minimum Delay Model. The green ratios for movements 2, 6, 4, and 8 estimated by the Hybrid Model are roughly the same as those estimated by MITSIM-Lab.

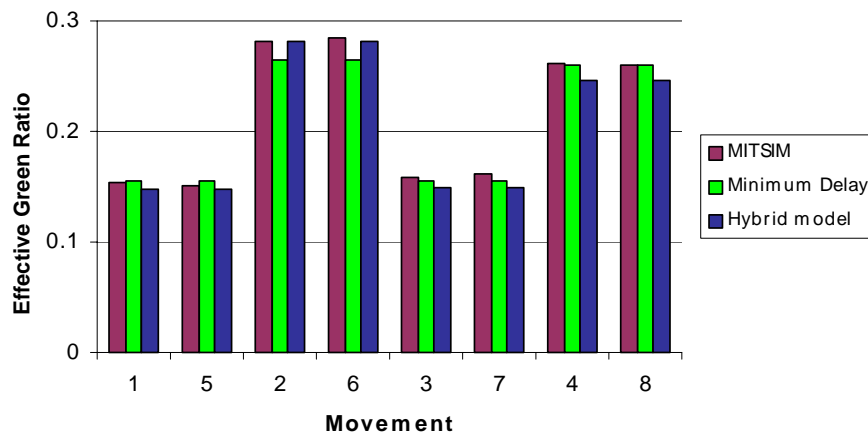


**Figure 5.4 Normal Traffic Volume**

The green ratios for all movements simulated by MITSIM-Lab are higher than those estimated by the Minimum Delay Model with light demand (shown in Table 5-5 and Figure 5.5). The difference for movements 1, 5, 3, 7, 4, and 8 are within 0.04. However,

the difference for movements 2 and 6 is 0.14. The demand from lane groups 2 and 6 are relatively higher than that from all other lane groups. In MITSIM-Lab simulation, the signal runs at the maximum green time for lane groups 2 and 6. However, the Minimum Delay Model estimates that the signal does not run at the maximum green time for lane groups 2 and 6. The difference can be explained by the fact that the saturation flow rate of a lane group is not simply addition of saturation flows of the lanes belonged to the lane group. Because of the interaction of the adjacent traffic, the saturation flow rate of the group is lower than 3 times the saturation flow rate for each lane. MITSIM-Lab simulates the vehicle movements at the intersection and also takes into account the interactions of vehicles between the adjacent lanes. However, we do not consider this factor when adjusting the saturation flow rates for Lane Groups 2 and 6. The Hybrid Model estimates slightly higher green ratios for the left-turn movements 1, 5, 3, and 7 than MITSIM-Lab and estimates slightly lower green ratios for the through movements 2, 6, 4, and 8. However, the differences are within 0.04. Therefore, the Hybrid Model estimates roughly the same green ratios for all lane groups as those simulated in MITSIM-Lab.

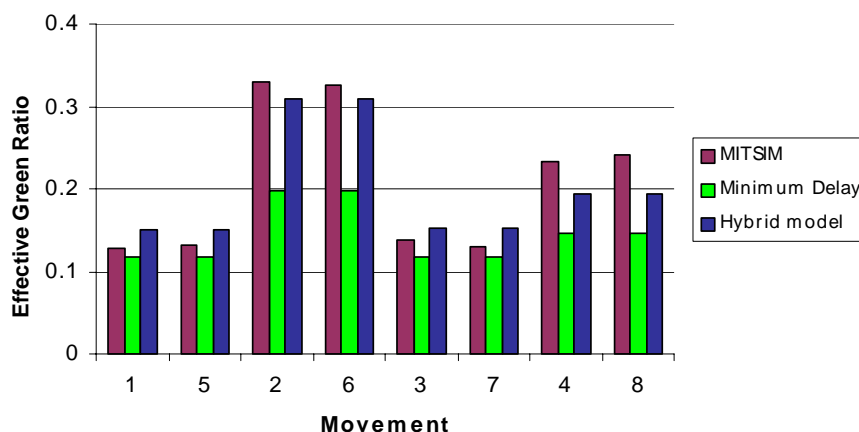


**Figure 5.5 Light Traffic Volume**

The green ratios for movements 2 and 6 estimated by the two proposed models with normal demand are slightly higher than those for the same movements with heavy demand. The results are reasonable because the green ratio is not a linear function of the ratio of flow rate to the saturation flow rate on its approach. When we reduce the demand proportionally, we can satisfy the demand on approaches 2 and 6 at the expense of increasing delay on other approaches. In turn green ratio on approaches 2 and 6 is relatively higher than that on approaches 2 and 6 when the intersection runs at maximum green times. The phenomena exist in real the world with highly congested networks. When demand exceeds the supply capacity and all phases run at maximum green, some approaches with relatively high demand are not given the green times that is necessary for serving high demand. When the demand decreases, the approach with relatively higher demand gets higher green ratio.

#### 5.1.4 Comparison of the Green Time Estimations by Different Models at An Intersection with Permitted Left Turn Phases

We compare of the green time estimations from the proposed models with those from MITSIM-Lab simulation at the Isolated Intersection with Permitted Left-turn Phases (the Intersection of Pasteur and Laguna Canyon) in this sub-section. The comparison of the green times estimated by the Minimum Delay Model or the Hybrid Model with those simulated by MITSIM-Lab is conducted with three testing scenarios, i.e., heavy, normal, and light traffic volumes.

#### Adjustment of Flow Rates

The three test scenarios are listed in Table 5-6. We adjust left-turn turn volume and right-turn volume. The equivalent left-turn flow rates is computed by the method developed in Section 3.3, considering the conflicts between the permitted left-turn vehicles on Pasteur Street and the opposing through traffic. The equivalent flow rates are shown in Table 5-6. With high opposing through traffic, the adjustment factor of equivalent flow rate is high. For example, when the opposing flow rate is 933 vph, the adjustment factor for movement 4 is 4.15, while the adjustment factor for movement 8 is 2.14 when the opposing through flow rate is 630 vph. When Right Turn on Red (RTOR) is permitted, the right-turn vehicles on Pasteur are “shadowed” by the protected left-turn phases from the Laguna Canyon. Free-flowing right turn vehicles that are not under signal control are removed from the analysis. We remove 50 percent of the right turn vehicles from the input flow of each right-turn movement on Pasteur.

**Table 5-6 Flow Rates into the Intersection**

Movement	Orientation	Scenarios (veh/hr)		
		Heavy	Normal	Light
1	South LT	568	298	238
5	North LT	568	298	238
2	North Thr	2674	1678	1426
6	South Thr	2674	1678	1426
4	East Thr	933	530	504
	Left-turn	300	130	104
	Equivalent Left-turn	1245	278	197
8	West Thr	933	630	504
	Left-turn	300	130	104
	Equivalent Left-turn	1245	278	197

Note: Flow rate of through movement = flow rate of through movement + 0.5\*flow rate of right-turn movement

#### Comparison of Effective Green Ratios for Lane Groups

The effective green ratios for each phase group estimated with the Minimum Delay Model, the Hybrid Model and simulated in MITSIM-Lab are shown in Table 5-7. The comparison of effective green ratios estimated by the three models under different scenarios is presented as bar charts shown in Figure 5.6 to Figure 5.8.

**Table 5-7 Comparison of Effective Green Ratios Estimated by Different Models under Different Scenarios at the Intersection with Permitted Left-turn Phases**

Movement	Orientation	Heavy			Normal			Light		
		MITSIM	Minimum Delay	Hybrid	MITSIM	Minimum Delay	Hybrid	MITSIM	Minimum Delay	Hybrid
1	South LT	0.207	0.222	0.222	0.161	0.161	0.178	0.150	0.154	0.154
5	North LT	0.207	0.222	0.222	0.162	0.162	0.178	0.154	0.154	0.154
2	North Thr	0.448	0.444	0.444	0.461	0.461	0.461	0.452	0.500	0.500
6	South Thr	0.447	0.444	0.444	0.460	0.460	0.461	0.447	0.500	0.500
4	East Thr	0.221	0.222	0.222	0.239	0.239	0.240	0.241	0.199	0.199
8	West Thr	0.221	0.222	0.222	0.238	0.238	0.240	0.240	0.199	0.199
Cycle length (sec)		110	108	108	99	100	103	88	81	85
Simulation time (sec)		3583	3600	3600	3565	3600	3600	3578	3600	3600

Note: The green times and green ratios are average values of four runs.

The actuated signal operates at maximum green times simulated by MITSIM-Lab with heavy demand as shown in Table 5-7 and Figure 5.6. The effective green ratios for all the lane groups estimated by the Minimum Delay Model and the Hybrid Model are roughly the same as those simulated by MITSIM-Lab.

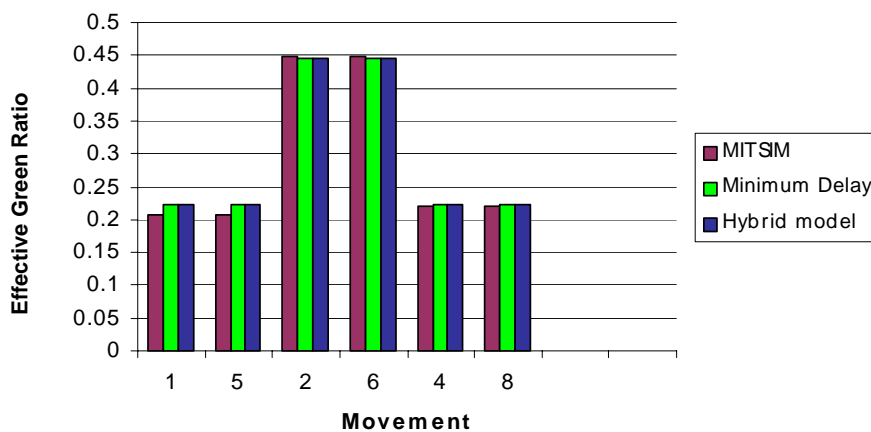


**Figure 5.6 Heavy Traffic Volume**

The green ratios for all movements simulated by MITSIM-Lab are approximately the same as those estimated by the Minimum Delay Model with normal demand as shown in Table 5-7 and Figure 5.7.

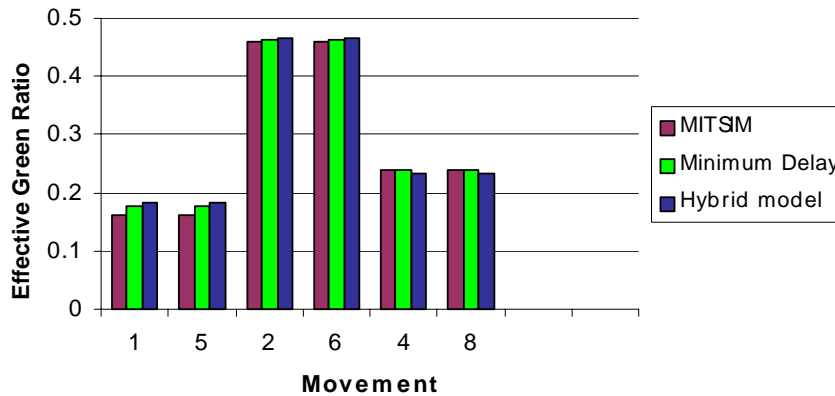


**Figure 5.7 Normal Traffic Volume**

The green ratios for movements 1 and 5 simulated by MITSIM-Lab are roughly the same as those estimated by the Minimum Delay Model with light demand as shown in Table 5-7 and Figure 5.8. The Minimum Delay Model estimates slightly higher effective green ratios for movements 2 and 6 than MITSIM-Lab and slightly lower effective green ratios for movements 4 and 8 than MITSIM-Lab. The Hybrid Model estimates approximately the same green ratios for movements 1 and 5 as those simulated by the MITSIM-Lab. The Hybrid Model estimates higher green ratios for the through movements 2 and 6 than MITSIM-Lab and estimates lower green ratios for the movements 4 and 8 than MITSIM-Lab. We do not use left-turn factor when adjusting the saturation flow rates of the approaches with the permitted left-turn. The saturation flow rates for the two approaches with permitted phases are biased upward. Thus the approaches with permitted left-turn phasing get relatively less effective green times. However, this problem should be resolved if the left-turn saturation flow rates are adjusted properly.

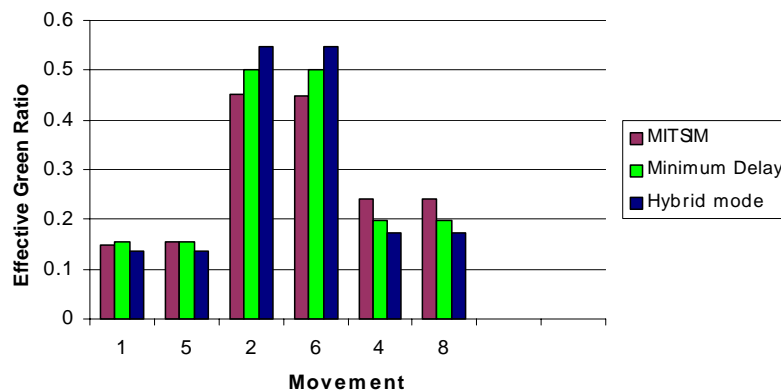


**Figure 5.8 Light Traffic Volume**

## 5.2 Validation of the Capacity Estimation Models at Network Level

### 5.2.1 Introduction

The validity of the Hybrid Model and the Minimum Delay Model was tested using field data from Irvine, CA. A real road network with two interstate highways and four arterial roads, which is shown in Figure 5.9, is used to validate the proposed capacity estimation models. The network has eighty signal-controlled intersections among which thirty intersections have actuated controls. The field observations include vehicle occupancies and vehicle counts at sensors in arterial roads at every 5-minute interval and at sensors in freeways at every one-minute interval for 24 hours per day. The data are used to calibrate the main parameters of DynaMIT and to evaluate the performance of the capacity estimation models.

We randomly selected fifteen isolated intersections with fully actuated control and with protected phases. The Hybrid Model and the Minimum Delay Model are used to dynamically estimate the capacity of lane groups of those fifteen intersections. The capacities at all the other intersections are statically estimated using method in the HCM. Traffic from 4:30 am to 8:15 am is simulated. In the first test, the Hybrid Model is used to estimate the time-dependent capacities of lane groups of those selected intersections in DynaMIT. In the second test, the Minimum Delay Model is used to estimate the capacities of lane groups of those intersections. The simulated flows at all sensors are compared to those predicted by DynaMIT with static capacity estimation by the HCM method.

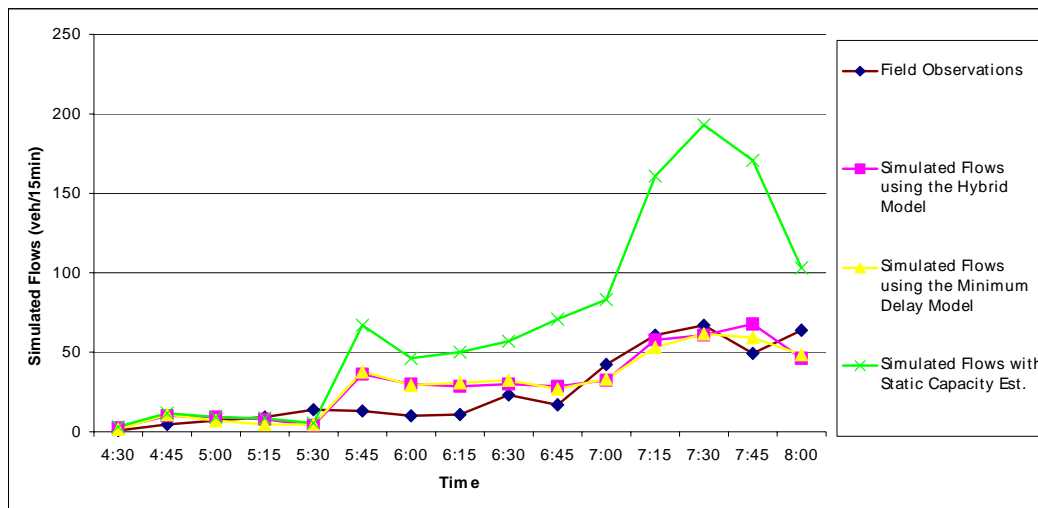


Figure 5.9 Irvine Road Network

### 5.2.2 Comparison of the Field Observations and the Simulated Flows

We compare the traffic volumes simulated by DynaMIT with the real observations to evaluate the performance of the proposed capacity estimation models. We show the comparison of the simulated flows and the field observations from 4:30 – 8:15 am at two sensors.

The simulated sensor flows and field observations at sensors 46 and 47 close to the intersection of Sand Canyon and Alton Street are shown in Figure 5.10 and Figure 5.11. The traffic counts at the sensors are accumulated flows for every 15-minute interval starting at 4:30 and ending at 8:15 am. The traffic counts at each sensor simulated by DynaMIT with both the Hybrid Model and the Minimum Delay Model are closer to the field observations than those simulated by DynaMIT with static capacities estimated by method in the HCM. Figure 5.10 shows that DynaMIT with static capacity estimation overestimates the simulated flows during morning rush hour, 7:00-8:00 am whereas the same software with the dynamic capacity estimation by the Hybrid Model and the Minimum Delay Model predicts the traffic volumes for the morning rush hour, which is close to the field observations. Figure 5.11 shows that DynaMIT with static capacity estimation underestimates the simulated flows during morning rush hour. Although DynaMIT with the dynamic capacity estimation by the Hybrid Model and the Minimum Delay Model also underestimates the traffic volumes for the interval from 7:30 to 7:45 am, it predicts the simulated traffic volumes which are closer to the field observations than those predicted by DynaMIT with static capacity estimation.



**Figure 5.10 Field Observations v.s. Simulated Flows at Sensor 46**

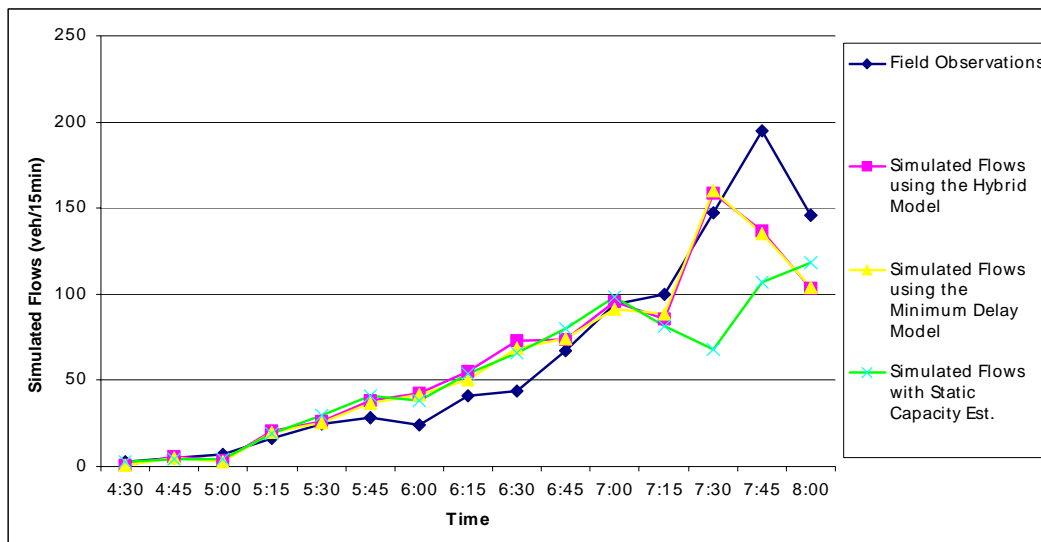


Figure 5.11 Field Observations v.s. Simulated Flows at Sensor 47

With the Hybrid Model and the Minimum Delay Model, capacities of lane groups of intersections are estimated by aggregated traffic flows in every five-minute-interval at the fifteen selected intersections. Since the estimated capacities are functions of time-dependent flow rates the capacity estimation reflects the with-in day traffic dynamics. Therefore, the simulated traffic volumes are closer to the field observations than those predicted by DynaMIT with static capacity estimation.

### 5.2.3 Error Statistics

The Root Mean Square Error (RMS) of the simulated flows at 59 sensors during morning rush hour is computed for validating the Hybrid Model and the Minimum Delay Model.

$$\text{RMS} = \sqrt{\frac{\sum_1^N (y_i - \hat{y}_i)^2}{N}}$$

where  $y_i$  and  $\hat{y}_i$  are field observations and simulated traffic volumes, respectively.

Root Mean Square Errors of average simulated flow rates from 7:00 to 8:00 am for seven runs with static lane group capacities was 202.6 veh/hr, while with capacities estimated by the Hybrid and the Minimum Delay Models were 183.9 and 185.8 veh/hr, respectively. The total traffic volume at all the sensors is 103,590 vehicles/hour. RMS of the flows simulated by DynaMIT with lane group capacities estimated by the Hybrid Model is lower than that simulated by DynaMIT with static lane group capacities. So is RMS for the flows simulated by DynaMIT with the lane group capacities estimated by the Minimum Delay.

### 5.3 Validation Conclusion

The experimental results of effective green ratios simulated by MITSIM-Lab and estimated by the two proposed models at the two intersections in Irvine, CA demonstrate that the Minimum Delay Model and the Hybrid Model estimate roughly the same effective green ratios as those simulated by MITSIM-Lab except that the Minimum Delay Model estimates slightly lower green ratios when the traffic volumes are light at the intersections. With only the flow rates of the lane groups of an intersection, the Minimum Delay Model provides green time estimations that are roughly close to those simulated by MITSIM-Lab. The Hybrid Model provides estimates close to those simulated by MITSIM-Lab because it is based on more intersection-specific information such as unit extensions, minimum and maximum green times, speed limits on the approaches to the intersection, and length of the detectors in each roadway.

Flows at sensors simulated by DynaMIT with capacities estimated by both the Hybrid Model and the Minimum Delay Model are closer to the observations than those simulated by DynaMIT with static capacity estimation at network level. The root mean square errors of the flow rates estimated by DynaMIT with the proposed models are lower than those by DynaMIT using static capacity estimation. The comparisons of simulated flow rates and field observations at network level illustrate that the Minimum Delay Model and the Hybrid Model predict more accurate lane group capacities than the static capacity estimation method in HCM 1994.

## Chapter 6 Conclusion and Future Study

### 6.1 Conclusion

The Minimum Delay Model needs only flow rates to estimate the capacities of lane groups at an intersection. However, the model requires more computation than the Hybrid Model since it determines the parameters by an iterative numerical algorithm. This model is appropriate for capacity estimation of intersections with adaptive control since the Minimum Delay Model minimizes the total delay at the intersections. Because the model is developed based on the assumption that queues dissipate during the end of the cycle, the Minimum delay model is not appropriate for intersections with over-saturated traffic flows.

The Hybrid Model requires information of the unit extensions, detector lengths, speed limits of the approaches, and the maximum green times of each phase to estimate the green extension periods. It is an improved version of the model in HCM 2000. Unlike the HCM model, the Hybrid does not need an iterative procedure to estimated lane group capacities since it has a closed form expression for queue service time. Therefore, the Hybrid Model is more appropriate for capacity estimation of intersections with actuated control in dynamic traffic assignment than the HCM 2000 model, and works well in both rash hour and non-rush hours. However, the requirements of intersection specific data sometimes limit the applicability of the Hybrid Model since those data are not always available. In addition, the accuracy of the Hybrid Model also depends on the quality of those input data.

Both the Minimum Delay Model and the Hybrid Model are implemented in DynaMIT. For planning purposes, if detailed information of signal timing plans is not available, the Minimum Delay Model is more appropriate than the Hybrid Model since computation time is not a major concern in the application for transportation planning. Although the Minimum Delay Model requires more computation, we can overcome the shortcomings of this model by using the same parameters for the entire simulation interval. The Hybrid Model needs less computation than the Minimum Delay Model because it has closed form expressions for queue service time and green time extension. The model is more applicable than the Minimum Delay Model in real-time dynamic traffic assignment. Since the Minimum Delay Model and the Hybrid Model estimate the capacities of lane groups of intersections by the time-dependent traffic volumes in every capacity update interval, the capacity estimations reflect within-day traffic dynamics.

Since actuated controllers extend the green times based on the arrivals of traffic, the green extension period should not be ignored. The Minimum Delay Model has parameters capturing the green extension periods in the cycle length and green time expressions and the Hybrid Model explicitly estimates the green extension based on an analytical model. Therefore, both the Minimum Delay Model and the Hybrid Model are theoretically superior to Webster's and the TCS Handbook model for actuated control in estimating capacity of intersections with actuated control. The Minimum Delay Model and the Hybrid Model are sensitive to the value of the total lost time, which is an input

parameter. The value of the total lost time must be carefully determined, otherwise the above two models will give incorrect capacity estimations. The Hybrid Model is also sensitive the unit extension, which is a parameter of the signal timings.

## 6.2 Future Study

In this research, we directly formulate the traffic control in the mesoscopic traffic simulator for dynamic traffic assignment. DTA model assigns OD demands onto the network with capacity constraints on each lane group while the lane group capacities are estimated by the Minimum Delay Model or the Hybrid Model based on the simulated traffic volumes. Since the capacities of lane groups and the simulated traffic volumes are inter-dependent, the interactions between traffic control strategies and drivers' route choice should be studied.

The dynamic traffic assignment and traffic control can be formulated as two-level programming. One level is the traffic control problem that minimizes the total delay at each intersection. The other level of the optimization problem is traffic assignment with the lane group capacities as input data from the traffic control problem. The framework of combined dynamic traffic assignment and traffic control is presented in Figure 6.1. Solution algorithms should be studied for determining the capacities of intersections and traffic assignment in network with adaptive or actuated control. In DynaMIT, we use the simulated flow rates estimating the capacity of lane groups. The estimated capacities are used in determining the traffic assignment on the network.

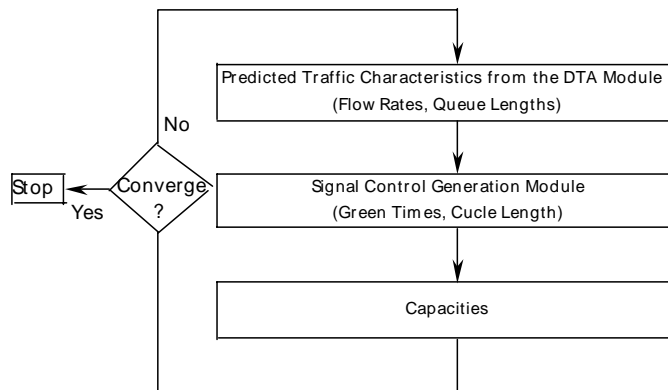


**Figure 6.1 Interactions of Signal Control with DTA**

## Appendix A Green Times and Cycle Length for N Phases

### 1. The Relationship between $\lambda_2$ , and $y_2$ for Approach 2

Total number of arrivals on approach 2 = total number of departures on approach 2:

$$(\bar{G}_1 + \bar{G}_2 + L)\bar{q}_2 = \bar{G}_{2,q} s_2 + \bar{G}_{2,e} \bar{q}_2 \quad (\text{A-1})$$

where

$$\bar{C} = \bar{G}_1 + \bar{G}_2 + L \quad (\text{A-2})$$

Substituting Equation (A-2) for  $\bar{C}$  into Equation (A-1), we have

$$\bar{C} \bar{q}_2 = \bar{G}_{2,q} s_2 + \bar{G}_{2,e} \bar{q}_2$$

Dividing both sides of Equations (A-2) by  $\bar{q}_2$ , we have

$$\bar{C} = \bar{G}_{2,q} \frac{1}{y_2} + \bar{G}_{2,e} \quad (\text{A-3})$$

where

$$y_2 = \bar{q}_2 / s_2. \quad (\text{A-4})$$

Let  $\alpha_2$  be the ratio of green extension period of Phase 2 to queue service time of the same phase.

$$\bar{G}_{2,e} = \alpha_2 \bar{G}_{2,q}. \quad (\text{A-5})$$

Substituting Equation (A-5) for  $\bar{G}_{2,e}$  into Equation (A-3) yields

$$\bar{C} = \bar{G}_{2,q} \frac{1}{y_2} + \alpha_2 \bar{G}_{2,q}$$

Dividing both sides of the above equation by  $\bar{C}$ , we have

$$1 = \frac{\lambda_2}{y_2} + \alpha_2 \lambda_2 \quad (\text{A-6})$$

where

$$\lambda_2 = \bar{G}_{2,q} / \bar{C}. \quad (\text{A-7})$$

### 2. The Cycle Length and Green Times for An Intersection with n Phase Groups

We derive the cycle length formulation for a general case where an intersection is controlled by an actuated traffic light with  $n$  phase groups. Each phase group controls a set of lane groups, which are shown green indication concurrently. Assume that Lane Group  $i$  is the representative lane group of phase group  $i$ , i.e., the ratio of flow rate to the saturation flow rate is the highest among the lane groups in this phase group.

The total number of arrivals on lane group  $i$  = the total number of departures on lane group  $i$

$$(\bar{G}_1 + \dots + \bar{G}_n + L)\bar{q}_i = \bar{G}_{i,q} s_i + \bar{G}_{i,e} \bar{q}_i \quad (\text{A-8})$$

where

$$\bar{C} = \sum_{i=1}^n \bar{G}_i + L \quad (\text{A-9})$$

Substituting Equation (A-9) for  $\bar{C}$  into equation (A-8) yields

$$\bar{C} \bar{q}_i = \bar{G}_{i,q} s_i + \bar{G}_{i,e} \bar{q}_i, \text{ for } i = 1, \dots, n. \quad (\text{A-10})$$

Dividing both sides of Equations (A-10) by  $\bar{q}_i$ , we have

$$\bar{C} = \bar{G}_{i,q} \frac{1}{y_i} + \bar{G}_{i,e}, \text{ for } i = 1, \dots, n \quad (\text{A-11})$$

where

$$y_i = \bar{q}_i / s_i, \text{ for } i = 1, \dots, n. \quad (\text{A-12})$$

Let  $\alpha_i$  be the ratio of green extension period of phase group  $i$  to queue service time of the same phase group.

$$\bar{G}_{i,e} = \alpha_i \bar{G}_{i,q}, \text{ for } i = 1, \dots, n. \quad (\text{A-13})$$

Substituting Equation (A-13) into Equation (A-11), we have

$$\bar{C} = \bar{G}_{i,q} \frac{1}{y_i} + \alpha_i \bar{G}_{i,q}. \quad (\text{A-14})$$

Dividing both sides of Equation (A-14) by  $\bar{C}$ , we have

$$1 = \lambda_i \frac{1}{y_i} + \alpha_i \lambda_i \quad (\text{A-15})$$

where

$$\lambda_i = \bar{G}_{i,q} / \bar{C}. \quad (\text{A-16})$$

From Equation (A-15), we represent  $\lambda_i$  in terms of  $y_i$  and  $\alpha_i$

$$\lambda_i = \frac{1}{\left(\alpha_i + \frac{1}{y_i}\right)} = \frac{y_i}{\alpha_i y_i + 1}. \quad (\text{A-17})$$

The average cycle length during a short time interval,  $T$ , equals the summation of the average green times allocated to phases group  $i$ , for  $i = 1, \dots, n$ , plus the total lost time during a cycle. That is, for the intersection

$$L + \sum_i^n \bar{G}_i = \bar{C}. \quad (\text{A-18})$$

The green duration for phase group  $i$  equals the time for the queue to dissipate,  $\bar{G}_{i,q}$ , plus the green extension period of phase group  $i$ ,  $\bar{G}_{i,e}$ , for  $i = 1, \dots, n$ . Substitute  $\bar{G}_{i,q} + \bar{G}_{i,e}$  for  $\bar{G}_i$  into the above equation,

$$L + \sum_i^n (\bar{G}_{i,q} + \bar{G}_{i,e}) = \bar{C}. \quad (\text{A-19})$$

Substituting Equation (A-13) for  $\bar{G}_{i,e}$  into the above equation yields

$$L + \sum_i^n (\bar{G}_{i,q} + \alpha_i \bar{G}_{i,q}) = \bar{C}.$$

Dividing both sides of the above equation by  $\bar{C}$ , we have

$$\begin{aligned} \frac{L}{\bar{C}} + \sum_i^n (1 + \alpha_i) \lambda_i &= 1 \\ \frac{L}{\bar{C}} &= 1 - \sum_i^n (1 + \alpha_i) \lambda_i \\ \bar{C} &= \frac{L}{1 - \sum_i^n (1 + \alpha_i) \lambda_i}. \end{aligned} \quad (\text{A-20})$$

After we determine the average cycle length, we need to determine the green time allocation for each phase group. By definition (referring to Figure 3.3), we have

$$\bar{G}_i = \bar{G}_{i,q} + \bar{G}_{i,e} = \bar{G}_{i,q} + \alpha_i \bar{G}_{i,q} = (1 + \alpha_i) \bar{G}_{i,q} \quad (\text{A-21})$$

Combining Equations (A-16) and (A-17), we have

$$\bar{G}_{i,q} = \frac{y_i}{1 + \alpha_i y_i} \bar{C}.$$

Substituting the above equation for  $\bar{G}_{i,q}$  into Equation (A-21), we have

$$\bar{G}_i = (1 + \alpha_i) \frac{y_i}{1 + \alpha_i y_i} \bar{C}. \quad (\text{A-22})$$

The Equation (A-13) can be rewritten as

$$\alpha_i = \bar{G}_{i,e} / \bar{G}_{i,q} \quad (\text{A-23})$$

$\alpha_i$  is a lane group specific parameter which is a function of  $y_i, q_i / s, \sum_i q_i / s$ , etc.

$$\alpha_i = f(y_i, q_i / s, \sum_i (q_i / s)). \quad (\text{A-24})$$

### 3. Correctness of the Minimum Delay Model

Consider Figure A.1, which depicts the cumulative arrival and departure curves for vehicles on approach  $i$ . Starting at an instant ( $t = 0$ ) when the queue on approach  $i$  does not exist, vehicles begin to accumulate on approach  $i$  during the red time  $R_i$ . At time  $t =$

$R_i$ , which is presented by point A, the signal turns green and a lost time of duration  $L_i$  begins. At time  $t = R_i + L_i$ , presented by point B, the queue on the approach begins to dissipate. After a duration of  $G_{i,q,real}$ , represented by point C, the queue has vanished. During the queue service time  $G_{i,q,real}$ , the queue is discharged at  $s_l$  vehicles per hour. Vehicles arriving after time  $t = R_i + L_i + G_{i,q,real}$  do not stop. Thus, the vehicle departure rate equals the arrival rate during the period of length,  $G_{i,e,real}$ . After the duration of  $G_{i,e,real}$ , the green phase of approach  $i$  terminates, which represented by point D. This figure shows that the average arrival rate during the period when the queue exists on the approach is larger than the average arrival rate during the cycle and that the average arrival rate during the period when no queue is present is lower than the average arrival rate.

Let  $\bar{q}_i$  be the average arrival rate during the cycle of length,  $R_i + L_i + G_{i,q,real} + G_{i,e,real}$ . The straight line from the origin to point D with slope  $\bar{q}_i$  is the arrival curve assuming that vehicles arrive uniformly at rate  $\bar{q}_i$ . The line OD intersects the departure curve at point C while the actual arrival curve intersects the departure curve at point  $C_{real}$ . The Minimum Delay Model (see Section 3.1) underestimates the queue service time, but it overestimates the green extension time. The estimated queue service time and green extension period are  $G_{i,q}$  and  $G_{i,e}$ , respectively. However, the overall green time estimated by the Minimum Delay Model is still close to the real green time.

Figure A.2 shows a case where the average arrival rate during the period when the queue exists on the approach is lower than that during the cycle and the arrival rate during the period when the queue does not exist is larger than that during the cycle. In this case, the Minimum Delay Model underestimates the green extension period, but it overestimates the queue service time. However, the overall green time is correctly estimated by the Minimum Delay Model.

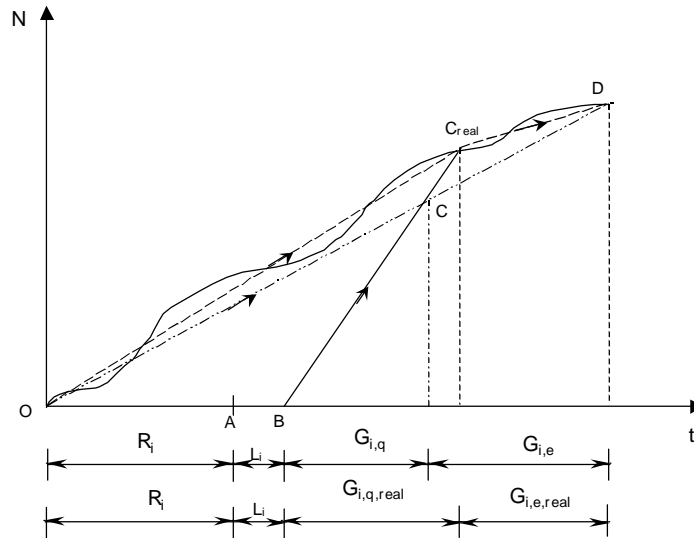


**Figure A.1 Traffic Actuated Control with Arrival Rate during Queue Service Time is Larger than the Average Arrival Rate**

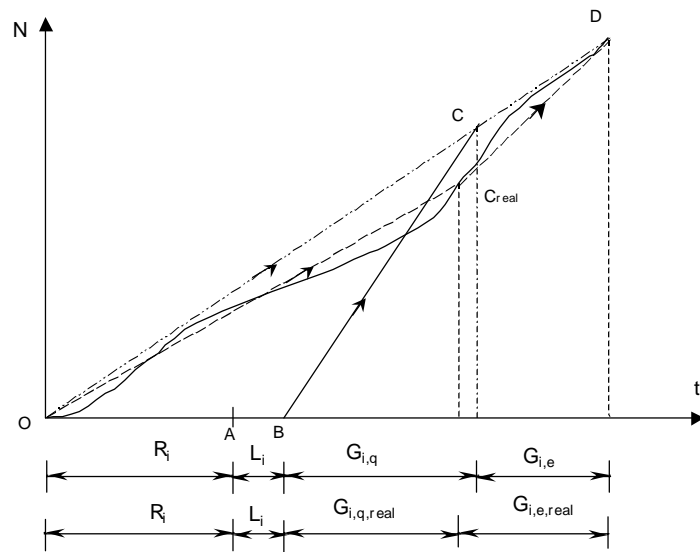


**Figure A.2 Traffic Actuated Control with Arrival Rate during Queue Service Time is Less than the Average Arrival Rate**

## Appendix B

### 1. Representation of $\bar{C}$ in Terms of $\alpha_1$ , $\alpha_2$ , $y_1$ , and $y_2$

Inserting Equations (3-31) and (3-33) into expression  $\sum_i (1 + \alpha_i) \lambda_i$ , we have

$$\sum_i (1 + \alpha_i) \lambda_i = \frac{(1 + \alpha_1) y_1}{\alpha_1 y_1 + 1} + \frac{(1 + \alpha_2) y_2}{\alpha_2 y_2 + 1} = \frac{(1 + \alpha_1) y_1 (\alpha_2 y_2 + 1) + y_2 (1 + \alpha_2) (\alpha_1 y_1 + 1)}{(\alpha_1 y_1 + 1) (\alpha_2 y_2 + 1)}$$

Substituting the above equation into the expression  $1 - \sum_i (1 + \alpha_i) \lambda_i$ , we have

$$\begin{aligned} 1 - \sum_i (1 + \alpha_i) \lambda_i &= 1 - \frac{(1 + \alpha_1) y_1 (\alpha_2 y_2 + 1) + y_2 (1 + \alpha_2) (\alpha_1 y_1 + 1)}{(\alpha_1 y_1 + 1) (\alpha_2 y_2 + 1)} \\ &= \frac{(\alpha_1 y_1 + 1) (\alpha_2 y_2 + 1) - (1 + \alpha_1) y_1 (\alpha_2 y_2 + 1) - y_2 (1 + \alpha_2) (\alpha_1 y_1 + 1)}{(\alpha_1 y_1 + 1) (\alpha_2 y_2 + 1)} \end{aligned} \quad (\text{B-1})$$

Let

$$\begin{aligned} A &= (\alpha_1 y_1 + 1) (\alpha_2 y_2 + 1) - (1 + \alpha_1) y_1 (\alpha_2 y_2 + 1) - y_2 (1 + \alpha_2) (\alpha_1 y_1 + 1) \\ &= 1 - (y_1 + y_2) - (\alpha_1 + \alpha_2) y_1 y_2 - y_1 y_2 \alpha_1 \alpha_2 \end{aligned} \quad (\text{B-2})$$

Substituting Equations (B-1) and (B-2) into Equation (3-28), we have

$$\bar{C} = L \frac{(\alpha_1 y_1 + 1) (\alpha_2 y_2 + 1)}{1 - (y_1 + y_2) - y_1 y_2 (\alpha_1 + \alpha_2) - \alpha_1 \alpha_2 y_1 y_2} = L \frac{(\alpha_1 y_1 + 1) (\alpha_2 y_2 + 1)}{A} \quad (\text{B-3})$$

### 2. Representation of $\bar{d}_u$ in terms of $\alpha_1$ , $\alpha_2$ , $y_1$ , and $y_2$

Substituting Equations (3-32) into the expression  $\bar{C} - \bar{G}_1$ , we have

$$\bar{C} - \bar{G}_1 = \bar{C} - \frac{y_1 (1 + \alpha_1)}{1 + \alpha_1 y_1} \bar{C} = \frac{1 + \alpha_1 y_1 - y_1 (1 + \alpha_1)}{1 + \alpha_1 y_1} \bar{C} = \frac{1 - y_1}{1 + \alpha_1 y_1} \bar{C} \quad (\text{B-4})$$

Similarly, substituting Equations (3-34) into the expression  $\bar{C} - \bar{G}_2$ , we have

$$\bar{C} - \bar{G}_2 = \bar{C} - \frac{y_2 (1 + \alpha_2)}{1 + \alpha_2 y_2} \bar{C} = \frac{1 + \alpha_2 y_2 - y_2 (1 + \alpha_2)}{1 + \alpha_2 y_2} \bar{C} = \frac{1 - y_2}{1 + \alpha_2 y_2} \bar{C} \quad (\text{B-5})$$

Substituting Equation (B-3) for  $\bar{C}$  into Equations (B-4) and (B-5), we get

$$\bar{C} - \bar{G}_1 = \frac{(1 - y_1)}{1 + \alpha_1 y_1} \frac{(\alpha_1 y_1 + 1) (\alpha_2 y_2 + 1)}{A} L = \frac{(1 - y_1) (\alpha_2 y_2 + 1)}{A} L \quad (\text{B-6})$$

$$\bar{C} - \bar{G}_2 = \frac{(1 - y_2)}{1 + \alpha_2 y_2} \frac{(\alpha_1 y_1 + 1) (\alpha_2 y_2 + 1)}{A} L = \frac{(1 - y_2) (\alpha_1 y_1 + 1)}{A} L \quad (\text{B-7})$$

Substituting Equations (B-6) and (B-7) for  $\bar{C}-\bar{G}_1$  and  $\bar{C}-\bar{G}_2$  respectively into Equation (3-6) and manipulating the equation, we obtain the two terms of Equation (3-6) as follows

$$\begin{aligned} \frac{T}{\bar{C}} \left[ \frac{1}{2} \bar{q}_1 (\bar{C}-\bar{G}_1)^2 \frac{1}{1-y_1} \right] &= \frac{T}{\bar{C}} \left[ \frac{1}{2} \bar{q}_1 \frac{1}{1-y_1} \left( \frac{1-y_1}{1+\alpha_1 y_1} \bar{C} \right)^2 \right] = T \left[ \frac{1}{2} \bar{q}_1 (1-y_1) \frac{\bar{C}}{(1+\alpha_1 y_1)^2} \right] \\ &= TD_1 \left[ \frac{\bar{C}}{(1+\alpha_1 y_1)^2} \right] \end{aligned} \quad (\text{B-8})$$

where

$$D_1 = \frac{1}{2} \bar{q}_1 (1-y_1) \quad (\text{B-9})$$

$$\begin{aligned} \frac{T}{\bar{C}} \left[ \frac{1}{2} \bar{q}_2 (\bar{C}-\bar{G}_2)^2 \frac{1}{1-y_2} \right] &= \frac{T}{\bar{C}} \left[ \frac{1}{2} \bar{q}_2 \frac{1}{1-y_2} \left( \frac{1-y_2}{1+\alpha_2 y_2} \bar{C} \right)^2 \right] \\ &= T \left[ \frac{1}{2} \bar{q}_2 (1-y_2) \frac{\bar{C}}{(1+\alpha_2 y_2)^2} \right] = TD_2 \left[ \frac{\bar{C}}{(1+\alpha_2 y_2)^2} \right] \end{aligned} \quad (\text{B-10})$$

where

$$D_2 = \frac{1}{2} \bar{q}_2 (1-y_2) \quad (\text{B-11})$$

Substituting the Equations (B-8) and (B-10) for the first term and the second term respectively into the Equation (3-6), we have

$$\begin{aligned} d_u &= TD_1 \frac{\bar{C}}{(1+\alpha_1 y_1)^2} + TD_2 \frac{\bar{C}}{(1+\alpha_2 y_2)^2} \\ d_u &= TD_1 \frac{1}{(1+\alpha_1 y_1)^2} L \frac{(\alpha_1 y_1 + 1)(\alpha_2 y_2 + 1)}{A} + TD_2 \frac{1}{(1+\alpha_2 y_2)^2} L \frac{(\alpha_1 y_1 + 1)(\alpha_2 y_2 + 1)}{A} \\ d_u &= \frac{TL}{A} \left[ D_1 \frac{\alpha_2 y_2 + 1}{\alpha_1 y_1 + 1} + D_2 \frac{\alpha_1 y_1 + 1}{\alpha_2 y_2 + 1} \right] \end{aligned} \quad (\text{B-12})$$

where A is defined in Equation (B-2)

### 3. Representation of $d_r$ in terms of $\alpha_1$ , $\alpha_2$ , $y_1$ , and $y_2$

From Equations (3-32) and (3-34), we have  $\frac{\bar{C}}{\bar{G}_1} = \frac{1+\alpha_1 y_1}{y_1(1+\alpha_1)}$  and  $\frac{\bar{C}}{\bar{G}_2} = \frac{1+\alpha_2 y_2}{y_2(1+\alpha_2)}$ .

Substituting the above Equation for  $\bar{C}/\bar{G}_i$  into Equation (3-8) for  $i = 1$  and  $2$ , we have

$$\rho_i = \frac{1 + \alpha_i y_i}{1 + \alpha_i} \quad (\text{B-13})$$

Substituting Equation (B-13) for  $\rho_i$  into expression  $\frac{\rho_i^2}{2(1 - \rho_i)}$ , we have

$$\frac{\rho_i^2}{2(1 - \rho_i)} = \frac{\left(\frac{1 + \alpha_i y_i}{1 + \alpha_i}\right)^2}{2\left(1 - \frac{1 + \alpha_i y_i}{1 + \alpha_i}\right)} = \frac{\left(\frac{1 + \alpha_i y_i}{1 + \alpha_i}\right)^2}{2\frac{\alpha_i(1 - y_i)}{1 + \alpha_i}} = \frac{(1 + \alpha_i y_i)^2}{2(1 + \alpha_i)\alpha_i(1 - y_i)} \quad (\text{B-14})$$

Substituting Equation (B-14) for the first term and the second term respectively into Equation (3-10), we obtain

$$d_r = T \left[ \frac{(1 + \alpha_1 y_1)^2}{2(1 + \alpha_1)\alpha_1(1 - y_1)} + \frac{(1 + \alpha_2 y_2)^2}{2(1 + \alpha_2)\alpha_2(1 - y_2)} \right] \quad (\text{B-15})$$

## Appendix C Input Data of Capacity Estimation

### 1. Determining Protected Left-turn or Permitted Left-turn Phases

The following description of the configuration of protected left-turn or permitted left-turn phases will help use to distinguish these two left-turn phases when we prepare input data for the capacity estimation.

Multi-phase control is used at intersections where one or more left-turns are determined to require protected phasing. Multi-phase control can be provided in a wide variety of ways, depending on the number of turns requiring protected phasing and the sequence and overlaps used. Modern traffic-actuated controllers implement a “dual-ring, concurrent” phasing in which each phase controls only one movement, but two phases are generally being displayed concurrently. Figure C.1 shows a concurrent dual-ring, which has eight phases. Phases 1 and 5, 3 and 7 are protected left-turn phases in ring 1 and ring 2, respectively.

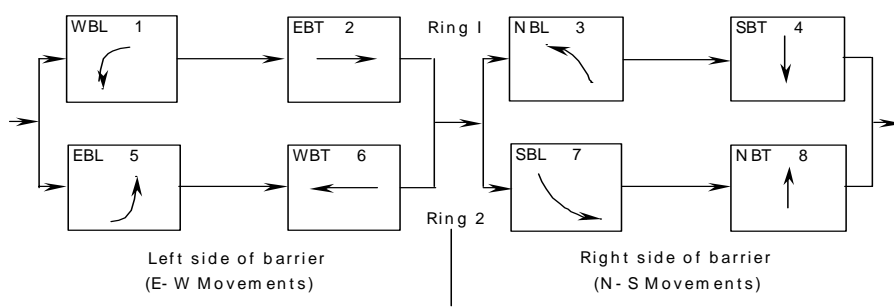


**Figure C.1 Dual-ring Concurrent Phasing Scheme with Assigned Movements**

Two-phase signalization is the most common form in use. If there are only two phases, the left-turns are on permitted phase. Each street receives one phase, with left turn and through movements being made on a permitted basis. Figure C.2 (a) shows simple two-phase operation. Both Phase 1 and Phase 2 have permitted left-turns. The left-turn flow rate, which is under control of permitted phase, should be converted to equivalent through flow rates in estimation of the capacity of the approach.

Three-phase operation provides protected turns on one street and four-phase operation provides protected turns on two streets. Figure C.2 (b) and (c) show simple three-, and four-phase configuration. Exclusive left-turn phases require that exclusive left-turn lanes be provided. Waiting left-turners do not block or delay through-vehicles on the approaches. The addition of exclusive left-turn phases for one or both intersecting streets generally leads to increased cycle lengths and increased delay. Under certain specified conditions (e.g., speed limit over 45 mph; left-turn must cross three or more opposing lanes; double left-turn lanes on the approach), protected-only phasing is preferable. The cycle lengths and green times are computed as multi-phase control.

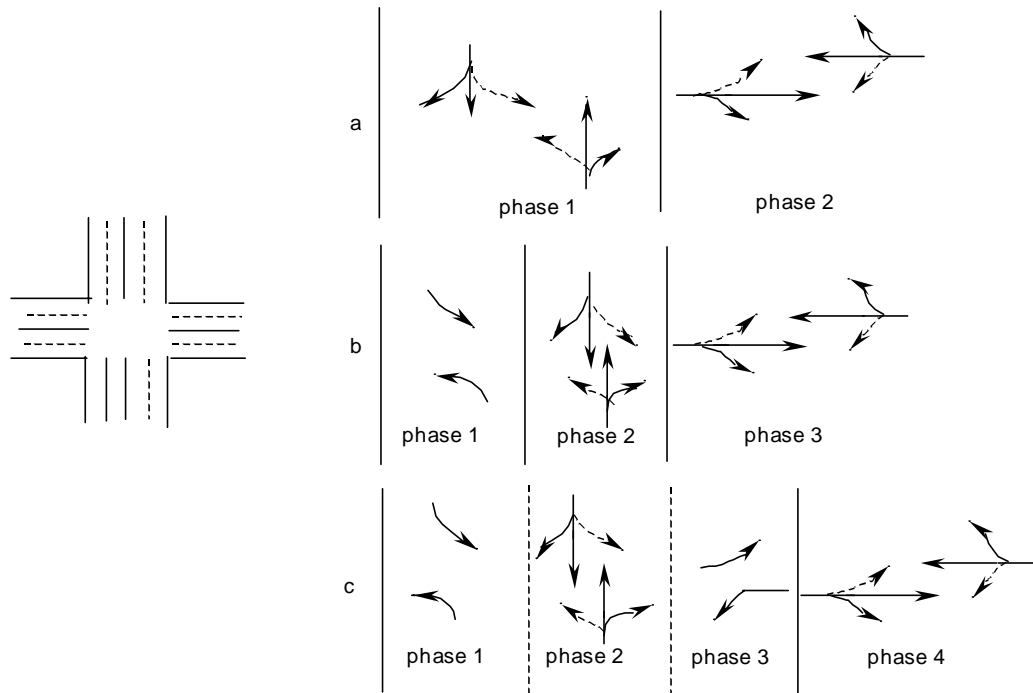


**Figure C.2 Illustration of Simple Two-, Three-, and Four-phase Operation**

## 2. Preparation of Input Data for Actuated Control

The green times and the cycle length of an actuated intersection is sensitive to the total lost time which is the sum of the lost time per phase and the all-red indication display after each phase. The values of the lost time per phase and the all-red time can be the same across intersections in an area. They are defined in the “Controller” section in the parameter file of DynaMIT. These parameters are:

- LostTimePerPhase** = the lost time per phase at an intersection in seconds;
- AllRedTime** = all-red indication displayed after each phase in seconds;
- YellowChangeInterval** = yellow change interval;
- RandonDiscountFacor** = define how much percentage of the random delay should be taken into account in the total delay;
- CapacityUpdateInterval** = how often should the lane group capacities be updated;

The phase plan comprises the number of phases to be used and the sequence that the actuated phases are implemented. An example of phase plan of an actuated intersection is shown in Figure 5.1. The signal controller itself has several operating parameters that must be specified for each phase. Some of the parameters such as initial interval, unit extension, maximum green, and all-red clearance are used in estimating the capacities of

lane groups at the intersection. The minimum green equals the sum of initial interval and the unit extension. Figure 5.1 also shows the signal timings of the intersection. The phase plan and controller settings are input as lane group specific data in the network file in DynaMIT. If a lane group is at an actuated intersection, the data field for this lane group is,

“lane group id,” “saturation flow rate,” “phase id,” “minimum green,” “maximum green”, “unit extension.”

For example, the lane group data for the west bound left-turn and through lane group of Irvine Center Drive are as follows,

{WB Left-turn laneGroupID 3610 1 8 24 3}

{WB Through laneGroupID 5474 6 13 32 5}.

If signal control at an intersection is actuated control, the node attribute field of this node is,

“node id,” “node type,” “node name”

where code of “node type” is 6 for a node with actuated control.

## Bibliography

- Akcelik, R. Analysis of vehicle-actuated signal operations. Australian Road Research Board. Working Paper WD TE 93/007, 1993.
- Akcelik, R. Estimation of Green Times and Cycle Time for Vehicle-Actuated Signals. Transportation Research Record 1457, 1994.
- Allsop, R. E. (1972). Estimating the traffic capacity of a signalized road junction. Transpn Res. 6(3), 245-255.
- Al-Malik, M., and Gartner, N. Development of a combined traffic signal control – traffic assignment model, Urban traffic Networks, edited by Gartner, N. and Improta, G. Springer Verlag, Berlin, 1995.
- Andrews, C. M., Elahi, S. M., and Clark, J. Evaluation of New Jersey Route 18 OPAC/MIST traffic-control system. 1603, 1997, pp. 150-155.
- Bell, M. G. H. (1995) Stochastic users equilibrium assignment in networks with queues, Transportation Research 29B, 125-137.
- Brilon, W. Recent developments in Calculation methods for unsignalized intersection in West Germany. Intersection Without Traffic Signals, Ed. W. Brilon, 1988.
- Clegg, J., Smith, M., Xiang, Y., and Yarrow, R. Bilevel programming applied to optimizing urban transportation. Transportation Research 35B, 2001, 41-70.
- Courage, K. G. (1998). Capacity analysis of traffic-actuated intersection. NCHRP Web Doc 10 Final Report, TRB, National Research Council, Washington D.C.
- Courage, and Wallace, TRANSYT-7F Users Guide, Volume 4 in a series: Methodology for optimizing signal timing, US DOT, FHWA, 1991.
- Daganzo, C. F. (1996). Fundamentals of Transportation and Traffic Operations. Pergamon, Elsevier Science Ltd, Oxford OX5 1GB, UK.
- Garber, N. J. and Hoel, L. A. (1997) Traffic and Highway Engineering. PWS Publishing Company, Boston, MA 02116.
- Gartner, N. H., et. al. Evaluation of optimization policies for adaptive control strategy, Transportation Research Record, 1324, 1991, pp. 105-114.
- Gartner, N. H. Demand-responsive decentralized urban traffic control, Part I: Single-intersection policies. Report DOT/RSPA/DPB-50/81/24/ U.S. Department of Transportation, 1982.

- Gartner, N., Tarnoff, P. J., and Andrews, C. M. Evaluation of optimized polices for adaptive control strategy. *Transportation Research Record*, 1324, 1991, pp. 105-114.
- Highway Capacity Manual, Transportation Research Board, National Research Council, Washington, D.C., 2000.
- Hiller, F. M. and Lieberman G. J., "Introduction to Operations Research", McGraw-Hill, 1995, pp 661-752.
- Kell, J. H. and Fullerton, I. J., *Manual of Traffic Signal Design*, 2<sup>nd</sup> edition, Institute of Transportation Engineers, 1991.
- Luk, J. Y. K. Two traffic-responsive area traffic control methods: SCAT and SCOOT. *Traffic Engineering and Control*, 1984, pp. 14~22
- McDonald, M. and Hounsell, N.B., Road traffic control: TRANSYT and SCOOT. In "Concise Encyclopedia of Traffic and Transportation Systems," M. Papageorgiou, Editor, Pergamon Press, 1991.
- McShane, W. R., and Ross, R. P., *Traffic Engineering*, Prentice Hall, Englewood Cliffs, 1990, New Jersey.
- Mcshane, W. R. and Roess, R. P. *Traffic Engineering*. Prentice-Hall, Inc. New Jersey 07632, USA, 1990.
- Mcshane, W. R. and Roess, R. P. *Traffic Engineering*. Prentice-Hall, Inc. New Jersey 07632, USA, 1990.
- Rakha, H., and Van Aerde, M. REALTRAN: An off-line emulator for estimating the effects of SCOOT. *Transportation Research Record*, 1494, 1995, pp. 124-128.
- Roberston, D., Lucas, C. F., Baker, R. T. Coordinating traffic signals to reduce fuel consumption, TRRL Report 934, 1980.
- Roberston, D. Research on the TRANSYT and SCOOT methods of signal coordination. *ITE Journal*, January, 1986, pp. 36-40.
- Smith, M. J. "Two new models for assessing urban traffic control and road pricing strategies," *Traffic Engineering and Control*, April 1992, pp 245-249.
- Smith, M. J. "Traffic Control and Traffic Assignment in a Signal-Controlled Network with Queuing", *Transportation and Traffic Theory*, edited by N. H. Gartner and N. H. M. Wilson, 1997.
- Smith, M. J., and Ghali, M. The dynamics of traffic assignment and traffic control: A theoretical study. *Transportation Research B*, 199-, 409-421.

Smith, M. J. and Ghali, M. O. Dynamic traffic assignment and dynamic traffic control, Transportation and Traffic Theory, Edited by M. Koshi, Elsevier Science Publishing Co., 1990.

Smith, M. J. (199-) The dynamics of traffic assignment and traffic control: A theoretical study. Transportation Research 24B, 409-422.

Traffic control systems handbook, FHWA-SA-95-0-32, U.S. Department of Transportation, 1996.

Webster, F. V. Traffic signal settings. Road Research Technical Paper No. 39, Department of Scientific and Industrial Research, Road Research Laboratory, 1958, London, U.K.